ARL TECHNICAL REPORT 60-333

LOW-DENSITY STAGNATION-POINT HEAT TRANSFER IN HYPERSONIC AIR FLOW

CHARLES E. WITTLIFF
MERLE R. WILSON

CORNELL AERONAUTICAL LABORATORY, INC.
BUFFALO, NEW YORK

FEBRUARY 1961

AERONAUTICAL RESEARCH LABORATORY
AIR FORCE RESEARCH DIVISION

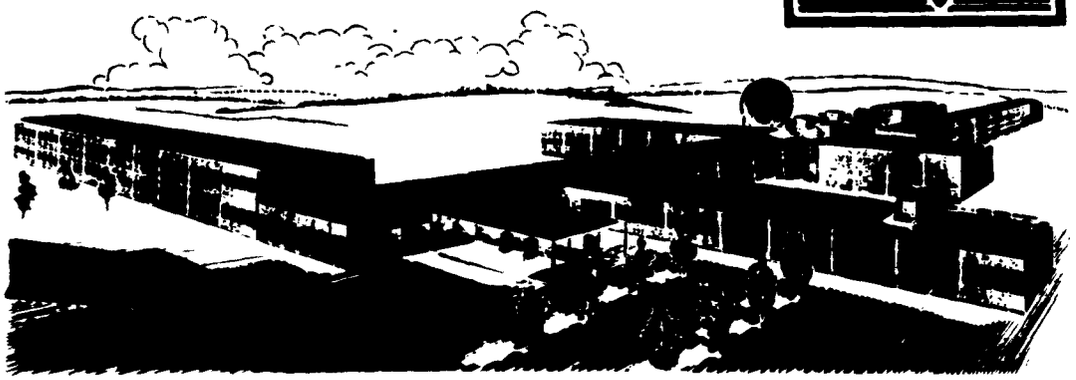

NOTICES

When Government drawings, specifications, or other data are used for any purpose other than in connection with a definitely related Government procurement operation, the United States Government thereby incurs no responsibility nor any obligation whatsoever; and the fact that the Government may have formulated, furnished, or in any way supplied the said drawings, specifications, or other data, is not to be regarded by implication or otherwise as in any manner licensing the holder or any other person or corporation, or conveying any rights or permission to manufacture, use, or sell any patented invention that may in any way be related thereto.

Qualified requesters may obtain copies of this report from the Armed Services Technical Information Agency, (ASTIA), Arlington Hall Station, Arlington 12, Virginia.

This report has been released to the Office of Technical Services, U. S. Department of Commerce, Washington 25, D. C. for sale to the general public.

Copies of ARL Technical Reports and Technical Notes should not be returned to Aeronautical Research Laboratory unless return is required by security considerations, contractual obligations, or notices on a specific document.

AF-WP-L-FEB 61 500

UNCLASSIFIED

Cornell Aeronautical Laboratory, Inc., Buffalo, N. Y.
LOW-DENSITY STAGNATION-POINT HEAT TRANSFER IN HYPERSONIC AIR FLOW, by C. E. Wittliff and M. R. Wilson. December 1960. 32p. illus., 51 refs. (Project 7064; Task 70169) (Report AF-1270-A-3; ARL-TR-60-333) (Contract AF 33(616)-6025) Unclassified report

A study of stagnation-point heat transfer to two- and three-dimensional bodies at low Reynolds numbers has been undertaken to obtain hypersonic low-density data and to demonstrate the suitability of the hypersonic shock tunnel as a facility for research in rarefied gasdynamics.

Low-density experiments have been made in air at Mach numbers from 8.4 to 11.6 in the CAL hypersonic shock tunnel. The stagnation pressure and temperature, as well as model diameter, were varied to obtain a range of Reynolds numbers from 11 to 1000, based on flow conditions behind the bow shock wave and model radius.

Circular-cylinder models having nominal diameters of 1/8, 1/4, and 1 inch were mounted transversely to the flow at the nozzle centerline. A hemisphere cylinder having a nominal diameter of 1/2 inch was mounted at the nozzle centerline with its axis

(over)

1. Aerodynamic Heating
2. Hypersonic Aerodynamics
3. Rarefied Air

I. Wittliff, C.E. and Wilson, M.R.
II. Aeronautical Research Laboratories Air Force Research Division
III. Contract AF 33 (616) -6025

UNCLASSIFIED

UNCLASSIFIED

Cornell Aeronautical Laboratory, Inc., Buffalo, N. Y.
LOW-DENSITY STAGNATION-POINT HEAT TRANSFER IN HYPERSONIC AIR FLOW, by C. E. Wittliff and M. R. Wilson. December 1960. 32p. illus., 51 refs. (Project 7064; Task 70169) (Report AF-1270-A-3; ARL-TR-60-333) (Contract AF 33(616)-6025) Unclassified report

A study of stagnation-point heat transfer to two- and three-dimensional bodies at low Reynolds numbers has been undertaken to obtain hypersonic low-density data and to demonstrate the suitability of the hypersonic shock tunnel as a facility for research in rarefied gasdynamics.

Low-density experiments have been made in air at Mach numbers from 8.4 to 11.6 in the CAL hypersonic shock tunnel. The stagnation pressure and temperature, as well as model diameter, were varied to obtain a range of Reynolds numbers from 11 to 1000, based on flow conditions behind the bow shock wave and model radius.

Circular-cylinder models having nominal diameters of 1/8, 1/4, and 1 inch were mounted transversely to the flow at the nozzle centerline. A hemisphere cylinder having a nominal diameter of 1/2 inch was mounted at the nozzle centerline with its axis

(over)

1. Aerodynamic Heating
2. Hypersonic Aerodynamics
3. Rarefied Air

I. Wittliff, C.E. and Wilson, M.R.
II. Aeronautical Research Laboratories Air Force Research Division
III. Contract AF 33 (616) -6025

UNCLASSIFIED

UNCLASSIFIED

Cornell Aeronautical Laboratory, Inc., Buffalo, N. Y.
LOW-DENSITY STAGNATION-POINT HEAT TRANSFER IN HYPERSONIC AIR FLOW, by C. E. Wittliff and M. R. Wilson. December 1960. 32p. illus., 51 refs. (Project 7064; Task 70169) (Report AF-1270-A-3; ARL-TR-60-333) (Contract AF 33(616)-6025) Unclassified report

A study of stagnation-point heat transfer to two- and three-dimensional bodies at low Reynolds numbers has been undertaken to obtain hypersonic low-density data and to demonstrate the suitability of the hypersonic shock tunnel as a facility for research in rarefied gasdynamics.

Low-density experiments have been made in air at Mach numbers from 8.4 to 11.6 in the CAL hypersonic shock tunnel. The stagnation pressure and temperature, as well as model diameter, were varied to obtain a range of Reynolds numbers from 11 to 1000, based on flow conditions behind the bow shock wave and model radius.

Circular-cylinder models having nominal diameters of 1/8, 1/4, and 1 inch were mounted transversely to the flow at the nozzle centerline. A hemisphere cylinder having a nominal diameter of 1/2 inch was mounted at the nozzle centerline with its axis

(over)

1. Aerodynamic Heating
2. Hypersonic Aerodynamics
3. Rarefied Air

I. Wittliff, C.E. and Wilson, M.R.
II. Aeronautical Research Laboratories Air Force Research Division
III. Contract AF 33 (616) -6025

UNCLASSIFIED

UNCLASSIFIED

Cornell Aeronautical Laboratory, Inc., Buffalo, N. Y.
LOW-DENSITY STAGNATION-POINT HEAT TRANSFER IN HYPERSONIC AIR FLOW, by C. E. Wittliff and M. R. Wilson. December 1960. 32p. illus., 51 refs. (Project 7064; Task 70169) (Report AF-1270-A-3; ARL-TR-60-333) (Contract AF 33(616)-6025) Unclassified report

A study of stagnation-point heat transfer to two- and three-dimensional bodies at low Reynolds numbers has been undertaken to obtain hypersonic low-density data and to demonstrate the suitability of the hypersonic shock tunnel as a facility for research in rarefied gasdynamics.

Low-density experiments have been made in air at Mach numbers from 8.4 to 11.6 in the CAL hypersonic shock tunnel. The stagnation pressure and temperature, as well as model diameter, were varied to obtain a range of Reynolds numbers from 11 to 1000, based on flow conditions behind the bow shock wave and model radius.

Circular-cylinder models having nominal diameters of 1/8, 1/4, and 1 inch were mounted transversely to the flow at the nozzle centerline. A hemisphere cylinder having a nominal diameter of 1/2 inch was mounted at the nozzle centerline with its axis

(over)

1. Aerodynamic Heating
2. Hypersonic Aerodynamics
3. Rarefied Air

I. Wittliff, C.E. and Wilson, M.R.
II. Aeronautical Research Laboratories Air Force Research Division
III. Contract AF 33 (616) -6025

UNCLASSIFIED

aligned with the flow. Thin-film resistance thermometers were used to measure the stagnation-point heat-transfer rate. The experimental heat-transfer rates are presented and compared with theoretical predictions. The data obtained with the transverse cylinder are in good agreement with continuum boundary-layer theory at all but the lowest Reynolds numbers. The hemisphere-cylinder data are in good agreement with theoretical analyses accounting for the presence of vorticity-interaction.

UNCLASSIFIED

UNCLASSIFIED

aligned with the flow. Thin-film resistance thermometers were used to measure the stagnation-point heat-transfer rate. The experimental heat-transfer rates are presented and compared with theoretical predictions. The data obtained with the transverse cylinder are in good agreement with continuum boundary-layer theory at all but the lowest Reynolds numbers. The hemisphere-cylinder data are in good agreement with theoretical analyses accounting for the presence of vorticity-interaction.

UNCLASSIFIED

UNCLASSIFIED

aligned with the flow. Thin-film resistance thermometers were used to measure the stagnation-point heat-transfer rate. The experimental heat-transfer rates are presented and compared with theoretical predictions. The data obtained with the transverse cylinder are in good agreement with continuum boundary-layer theory at all but the lowest Reynolds numbers. The hemisphere-cylinder data are in good agreement with theoretical analyses accounting for the presence of vorticity-interaction.

UNCLASSIFIED

UNCLASSIFIED

aligned with the flow. Thin-film resistance thermometers were used to measure the stagnation-point heat-transfer rate. The experimental heat-transfer rates are presented and compared with theoretical predictions. The data obtained with the transverse cylinder are in good agreement with continuum boundary-layer theory at all but the lowest Reynolds numbers. The hemisphere-cylinder data are in good agreement with theoretical analyses accounting for the presence of vorticity-interaction.

UNCLASSIFIED

UNCLASSIFIED

ARL TECHNICAL REPORT 60-333

LOW-DENSITY STAGNATION-POINT HEAT TRANSFER IN HYPERSONIC AIR FLOW

BY

CHARLES E. WITTLIFF
MERLE R. WILSON

CORNELL AERONAUTICAL LABORATORY, INC.
BUFFALO, NEW YORK

REPORT No. AF-1270-A-3
CONTRACT No. AF 33(616)-6025

FEBRUARY 1961

AERONAUTICAL RESEARCH LABORATORY
AIR FORCE RESEARCH DIVISION
AIR RESEARCH AND DEVELOPMENT COMMAND
UNITED STATES AIR FORCE
WRIGHT-PATTERSON AIR FORCE BASE, OHIO

McGregor & Werner, Inc., Dayton, O.
300 - October 1961 - 6-150 & 151

FOREWORD

The study on which this report is based constitutes a part of the research program on aero-thermo-characteristics of flight of hypersonic vehicles under the U.S. Air Force Contract AF 33(616)-6025, Project No. 7064 "Thermo-Aerodynamic Characteristics at Hypersonic Mach Numbers," Task No. 70169 "Research on Aerodynamic Flow Fields." The project is administered by the Fluid Dynamics Research Laboratory, Air Force Research Division, Wright-Patterson Air Force Base, with Mr. Robert D. Stewart acting as Task Scientist.

As indicated in the text, a portion of the work (the hemisphere-cylinder experiments and the theoretical work of H. K. Cheng) was performed under Contract Nonr 2653(00) with the U.S. Navy Office of Naval Research.

Some of the results contained in this report (the transverse-cylinder data) were presented in a talk entitled "Low-Density Research in the Hypersonic Shock Tunnel" given at the "Second International Symposium on Rarefied Gas Dynamics" held at the University of California, Berkeley, California from August 3 to 6, 1960. A written version of the talk will be published in the proceedings of the Symposium.

The authors wish to thank their colleagues in the Aerodynamic Research Department for their contributions to this program, particularly Dr. H. K. Cheng for the many consultations regarding his theoretical analysis. They would also like to acknowledge the assistance of Miss Eileen Stager who performed the detailed data reduction computations.

ABSTRACT

A study of stagnation-point heat transfer to two- and three-dimensional bodies at low Reynolds numbers has been undertaken at the Cornell Aeronautical Laboratory, Inc. The purpose of this investigation was to obtain hypersonic low-density data and to demonstrate the suitability of the hypersonic shock tunnel as a facility for research in rarefied gasdynamics.

Low-density experiments on a transverse cylinder and a hemisphere cylinder have been made in air at Mach numbers from 8.4 to 11.6 in the CAL 11- by 15-inch hypersonic shock tunnel. The stagnation pressure and temperature, as well as model diameter, were varied to obtain a range of Reynolds numbers from 11 to 1000, based on flow conditions behind the bow shock wave and model radius.

Circular-cylinder models having nominal diameters of 1/8, 1/4, and 1 inch were mounted transversely to the flow at the nozzle centerline. A hemisphere cylinder having a nominal diameter of 1/2 inch was mounted at the nozzle centerline with its axis aligned with the flow. Thin-film resistance thermometers were mounted along the stagnation line to measure the stagnation-point heat-transfer rate at one or more points along the cylinder and at the stagnation point on the hemisphere. The experimental heat-transfer rates are presented and compared with theoretical predictions. The data obtained with the transverse cylinders are in good agreement with continuum boundary-layer theory at all but the lowest Reynolds numbers and highest Knudsen numbers. The hemisphere-cylinder data indicated the presence of a significant vorticity-interaction effect. Good agreement with the theoretical analysis of H. K. Cheng accounting for this effect is indicated.

The success of these experiments in a shock tunnel that was not designed for low-density operation has led to a fuller investigation of the application of the shock tunnel to research studies of hypersonic, rarefied gasdynamics. The results of these considerations are discussed.

TABLE OF CONTENTS

TABLE OF CONTENTS (Contd.)

LIST OF ILLUSTRATIONS

NOMENCLATURE

C	Chapman-Rubesin linear viscosity-temperature coefficient, $C = \frac{\mu_*/\mu_0}{T_*/T_0}$
C_H	heat transfer coefficient, $C_H = q/\rho_\infty U_\infty (H_0 - H_W)$
H	enthalpy
k	parameter in Cheng's analysis, defined by Equation (2)
K	parameter in Cheng's analysis, defined by Equation (3)
Kn	Knudsen number
L	characteristic length
M	Mach number
p	pressure
Pr	Prandtl number
q	stagnation-point heat-transfer rate
R	radius
Re	Reynolds number
T	temperature
U	velocity
α	accommodation coefficient
γ	specific-heat ratio
δ	shock-wave thickness, Figure 1
Δ	shock-wave stand-off distance, Figure 1
ϵ	density ratio across a normal shock wave
ϵ'	parameter in Cheng's analysis, $\epsilon' = \rho_s/2\rho_s H_s$
λ	mean free path
μ	viscosity coefficient
ρ	density

Subscripts:

∞	free-stream flow conditions
b	body
o	free-stream stagnation conditions
s	flow conditions behind shock wave
w	flow conditions at the wall
os	stagnation-point conditions behind shock wave

INTRODUCTION

The phenomena encountered in hypersonic, rarefied-gas flows recently have been the object of an increasing number of investigations. Much of this interest has been stimulated by the prospect of manned-hypersonic vehicles. Because of the glancing re-entry trajectories and the requirements for sustained hypersonic flight, these vehicles will encounter rarefied-gasdynamic phenomena when they are flying at very high hypersonic speed and high altitudes. Hypersonic rarefied-gas flows have been treated theoretically in recent years; however, experimental low-density data has been confined mostly to Mach numbers of 6 or less (see for example, References 1, 2, 3). Because of its operating capability over a wide pressure range, it was felt that the shock tunnel could be used to obtain hypersonic low-density data. Consequently, a program of rarefied-flow studies has been undertaken at the Cornell Aeronautical Laboratory, Inc. utilizing the existing 11- by 15-inch hypersonic shock tunnel[4, 5]. The purpose of this program was twofold; first, to obtain hypersonic low-density data, and second, to investigate the shock tunnel as a hypersonic low-density research facility.

Stagnation-point heat transfer to two- and three-dimensional bodies was selected as the subject of the investigation both because it is of practical interest and has been treated theoretically by Probstein and Kemp[6], Herring[7], Hoshizaki[8], Ho and Probstein[9] and Ferri, Zakkay and Ting[10]. These theories indicate that the stagnation-point heat-transfer rate will be greater than that predicted by boundary-layer theory.

Transverse cylinders* having nominal diameters of 1/8, 1/4 and 1 inch, and a hemisphere cylinder having a diameter of 1/2 inch have been tested.

---

*The transverse-cylinder data were initially reported by the authors[11] at the Second International Symposium on Rarefied Gas Dynamics held at the University of California, Berkeley, California from August 3 to 6, 1960, and will be published in the proceedings of the Symposium.

Manuscript released by the authors December 15, 1960 for publication as an ARL technical report.

The experiments were made in air at Mach numbers from 8.4 to 11.6 and Reynolds numbers from 11 to 1000 based on flow conditions behind the bow shock wave and model radius. The stagnation temperatures ranged from 1500 to 2200°K and from 3200 to 3700°K. The Knudsen number based on mean free path behind the shock and body radius ranged from 4.8×10^{-4} to 3.6×10^{-2}.

These experiments have demonstrated the application of the shock tunnel to rarefied-gasdynamic research. It should be noted that the 11- by 15-inch shock tunnel, used in this program, was never designed for low-density studies. In fact, it has a two-stage nozzle with a rectangular cross-section, which is relatively poor for low-density flows with their associated thick nozzle-wall boundary layers. Nevertheless, no significant changes in operating techniques or instrumentation were required for the present program. The shock tunnel instrumentation developed in recent years proved entirely satisfactory for measuring pressures and heat-transfer rates. Based on the success of these experiments, a detailed study of the requirements for a hypersonic, low-density wind tunnel has been undertaken to explore additional applications of the shock tunnel to rarefied gasdynamic research.

In the present report, the various flow regimes between continuum and free-molecule flow, as classified by Hayes and Probstein[12], are described. Some of the pertinent theoretical solutions found for these regimes are indicated. In addition, a new theoretical treatment of viscous shock-layer flow by H. K. Cheng[13], which is used to correlate the hemisphere-cylinder data, is briefly discussed. Then the present experimental program is described. The results are compared with theoretical predictions and, for the hemisphere cylinder, with data obtained by Ferri, Zakkay, and Ting[10] in a conventional, blow-down wind tunnel. Next, the results of the study of low-density wind tunnel requirements are presented indicating that the shock tunnel possesses many advantages, some of them unique, that make it well suited for research in hypersonic rarefied gasdynamics. Finally, future shock tunnel developments which will enhance its capabilities for low-density research are described.

LOW-DENSITY FLOW PHENOMENA

It has been only during the past several years that studies of rarefied-gas flows have been extended to hypersonic speeds. For many years following the original work of Tsien[14], the regimes of rarefied gasdynamics were classified as "continuum flow," "slip flow," "transition flow," and "free molecule flow." Recently, Hayes and Probstein[12] have suggested a classification of hypersonic rarefied-gas flows as "boundary-layer regime," "vorticity-interaction regime," "viscous-layer regime," "incipient merged-layer regime," "fully-merged layer," "transitional layer regime," "first-order collision theory regime," and "free-molecule flow regime." These various regimes have been treated either in general or in detail in References 6, 9, 12, 15-18; however, the classification is still somewhat tentative.

As indicated by the references cited above, there is a growing body of literature devoted to the theory of hypersonic rarefied-gas flows. Experimental results for low-density flows at Mach numbers greater than 6 are relatively rare, however. References 19 and 20 report heat-transfer measurements to transverse cylinders at Mach numbers of about 6 and stagnation temperatures of about 300°K. Stagnation-point heat-transfer measurements at low Reynolds numbers on hemisphere cylinders at a Mach number of about 6 and stagnation temperatures from 4500°K to 6000°K have been reported in Reference 21. Similar measurements at Mach 8 and stagnation temperatures of 890°K and 1280°K are reported in Reference 10. Measurements of heat transfer to fine wires in free-molecule flow at Mach numbers from 10 to 18 are reported in Reference 22. These experiments were made in a hypersonic shock tunnel at stagnation temperatures from 1800°K to 2850°K. The latter three references and the present work constitute the only high-temperature, hypersonic, low-density data known to the authors. The experiments reported in References 10 and 21 are devoted to studying the vorticity interaction effects[12], while the experiments of Reference 22 deal with free-molecule flow about a transverse cylinder. The present study extends from the region of boundary-layer flow into the fully-merged layer regime.

Before describing the present experiments, the low-density phenomena encountered in the stagnation region of a blunt body at hypersonic speeds will be described. This description will also very briefly summarize the analyses contained in References 6-10, 12 and 15-18. The regimes, as previously cited, extend from continuum flow to free molecule flow as the density is decreased. The theoretical analysis of Cheng[13], which is presently available only as a C.A.L. memorandum, will be described separately.

Boundary-Layer Regime

At high Reynolds numbers viscous effects are restricted to a thin boundary layer, and the rest of the flow field between the body and the shock wave is inviscid. The classical boundary-layer theory (Navier-Stokes equations) for stagnation-point flows has been developed by Sibulkin[23], Reshotko and Cohen[24], Lees[25], Fay and Riddell[26] and others. Sibulkin's solution is for laminar, incompressible, low-speed flow about a body of revolution. The comparable solution for two-dimensional flow was obtained by Squire[27]. Of the various compressible boundary-layer theories, that of Fay and Riddell[26] is the most complete. Their analysis considers the case where the external inviscid flow may be dissociated and includes the effects of diffusion and atom recombination in the boundary layer. This analysis, which is applicable to both transverse cylinders and bodies of revolution, has been used for comparison of the present experimental results at the higher Reynolds numbers.

Vorticity-Interaction Regime

As the density and Reynolds number are lowered, the boundary-layer thickness increases until the vorticity in the inviscid flow begins to affect the boundary-layer structure. This vorticity is generated by the curved bow shock wave. The vorticity-interaction effect has been treated by Hayes and Probstein[12], Hoshizaki[8,21], and Ferri, Zakkay and Ting[10]. The first two analyses assume incompressible flow between the shock and the body, while the third analysis includes compressibility effects. A solution for this regime also results from Cheng's theory[13] which includes compressibility effects. In this regime the shock wave is assumed to be thin with negligible viscous

and heat conduction effects. It should be noted that for the transverse cylinder, the vorticity interaction is a second-order effect (in Reynolds number) while it is a first-order effect for the sphere or hemisphere cylinder[6].

Viscous-Layer Regime

At Reynolds numbers less than those required for the validity of the vorticity-interaction approach, the shock layer is a fully viscous contimuum region governed by the Navier-Stokes equations, and the shock wave is a discontinuity across which the Rankine-Hugoniot relations apply. The latter condition establishes a limit to this regime by requiring that the viscous shear be small compared to the tangential momentum transport across the shock wave.

Constant-density solutions have been obtained by Probstein and Kemp[6], Oguchi[17,28] and Hayes and Probstein[12]. Compressible flow solutions have been reported by Herring[7] and Ho and Probstein[9]. These analyses solve the Navier-Stokes equations using conditions behind the shock wave as the boundary conditions at the outer edge of a boundary-layer-type flow. These analyses are also restricted to the immediate neighborhood of the stagnation point.

Incipient Merged Layer Regime

Here the shock wave can no longer be considered as a discontinuity obeying the Rankine-Hugoniot relation, and the shock-layer flow is still considered as a continuum. Two possible approaches[12] are to consider the shock as a discontinuity obeying the conservation laws in which the viscous stresses and heat conduction are accounted for, or to use the complete Navier-Stokes equations to obtain a solution which includes the shock-wave structure and has free-stream conditions as outer boundary conditions. The latter approach is detailed by Probstein and Kemp[6], who present a numerical solution for the sphere.

Fully Merged Layer and Transitional Layer Regimes

This regime is bounded by the limits for the incipient merged layer regime and the first-order collision theory regime. The shock wave is no

longer a discontinuity and the shock layer is in either an almost continuum regime or an almost first-order collision regime. Accurate treatment of this flow regime requires the full formulation of kinetic theory. Failing this, Hayes and Probstein[12] suggest that the best approach, for engineering purposes, is to apply the complete Navier-Stokes equations. The limits of validity of this approach are unknown.

First-Order Collision Theory Regime

In this regime the Knudsen number, appropriately defined, is large, but not large enough for free-molecule flow concepts to be valid. This flow region can be analyzed by considering only collisions between free-stream molecules and molecules re-emitted from the surface. Such analyses have been made by Lunc and Lubonski[29], Baker and Charwat[30], Hammerling and Kivel[31], Liu[32], and Willis[33].

Free-Molecule Flow Regime

Here all intermolecular collisions are neglected and only the interaction of free-stream molecules with the surface is considered. There is a large body of literature on this subject. Recent general treatments of this flow regime are given, for example, by Schaaf and Chambre[34], Schaaf and Talbot[35], and Hayes and Probstein[12].

Low-Density Regime Boundaries

The limits of validity of these various regimes have been discussed in References 6, 12, 15, 16 and 18. For flow in the stagnation-point region of a blunt body they are given by Probstein[18] as follows:

Boundary Layer	$\frac{1}{\epsilon}\sqrt{\frac{\lambda_\infty}{R_b}} \ll 1$
Vorticity Interaction	$\lambda_s/R_b \ll \epsilon^2$
Viscous Layer	$\lambda_s/R_b \ll \epsilon^{3/2}$
Incipient Merged Layer	$\lambda_s/R_b \ll \epsilon$
Fully Merged Layer	$\lambda_s/R_b < \epsilon$
Transitional Layer	$\lambda_s/R_b > \epsilon$

First-Order Collision Theory $\lambda_w/R_b > 1$

Free-Molecule Theory $\frac{\lambda_\infty}{R_b} >> \frac{\sqrt{\pi\gamma}}{4}\sqrt{\frac{T_\infty}{T_w}}\, M_\infty$

where R_b is the body radius, ϵ is the density ratio across the shock wave, ρ_∞/ρ_s, and λ_∞, λ_s and λ_w are the mean free paths in the free-stream flow, behind the shock wave, and at the body, respectively. These regimes are shown in Figure 1 which is taken from Reference 18.

On the basis of these boundaries, the present experiments extend slightly into the fully merged layer regime for the transverse cylinder and up to the boundary between the incipient merged and fully merged layers for the hemisphere cylinder.

Low-Density Shock-Layer Theory of Cheng*

H. K. Cheng[13] has recently developed an approach to the hypersonic blunt-body problem utilizing the shock-layer concept and including viscous and heat-conduction effects in the shock layer as well as in the conservation relations of the shock itself. The work is as yet published only in Reference 13 which has a limited distribution. This investigation deals with flows in which the density is so low that the transport process may be as important as the convective process, but not so low that the continuum concept becomes invalid. Such an approach should be valid until the smallness of the density requires a kinetic theory treatment of the gas. The validity of the approach is further strengthened by the fact that the theory aggrees with free-molecule flow theory in the low-density limit. At present only the stagnation region for a body of revolution has been analyzed. It is planned to extend the study to two-dimensional flows.

Using this approach, Cheng has found that the problem may be separated into two regimes. In one regime, where the Rankine-Hugoniot shock relations hold, the vorticity-interaction theory of Hayes and Probstein[12]

*This work has been performed under the sponsorship of the U. S. Navy Office of Naval Research (Contract Nonr-2653(00)) and the U. S. Air Force Rome Air Development Center (Contract AF 30(602)-2267). The presentation here has been taken from Reference 13.

based on the boundary-layer approximation is found to be adequate even in the range of validity of viscous-layer theory. For the other regime, where the viscous and heat-conduction effects on the shock relations cannot be neglected, an analytic solution of the viscous shock layer has been obtained. This solution is subject to assumptions regarding the viscosity-temperature variation, the magnitude of $\epsilon' = \rho_s / 2\rho_s H_s$, and the order of $K^2 = \rho_\infty R_b / \mu_\infty C$ where C is the Chapman-Rubesin viscosity-temperature coefficient[36]. Also, a perfect gas with constant specific heats has been assumed. This solution is valid in the fully-merged layer regime.

As with the inviscid shock layer theory[37, 38], Cheng's analysis of the viscous shock layer requires a high shock compression ratio, which in turn requires a strong shock and a specific heat ratio not far from unity, i.e., $\epsilon' << 1$. The flow model, because of the simplicity resulting from the shock-layer concept, permits reduction of the problem to one comparable to that of the boundary-layer approximation. However, the formulation, which has been developed to within an error of order ϵ' , differs from the boundary-layer theory in that the normal pressure gradient is not generally negligible and in that the outer edge of the shock layer lies at a finite distance from the body surface. Implicit in the flow model is the continuum assumption since the compressible, Navier-Stokes equations are assumed to govern the flow.

The solutions obtained by Cheng will be compared with the present hemisphere-cylinder data as well as the data reported by Ferri et al[10].

EXPERIMENTS

Hypersonic Shock Tunnel

The C.A.L. 11- by 15-inch hypersonic shock tunnel[4] consists of a high-pressure driver tube 3.5 inches I.D. by 14 feet long, a driven tube 3 inches I.D. by 28 feet long, and a three-stage hypersonic nozzle (Figure 2) having a variable entrance area in the final stage. The driver and driven tubes are designed for 30,000 psi operation using either a single or double diaphragm between the two sections. The driven tube has instrumentation ports located at intervals along it as well as charging and charge pressure measuring ports. The driven tube is separated from the nozzle system by a Mylar diaphragm. Diaphragm thicknesses from 1/2 to 2 mils are used depending upon the initial driven tube charge pressure. The purpose of this diaphragm is to separate the two sections in order to maintain the proper driven tube pressure while permitting evacuation of the test section to promote efficient tunnel starting[39].

The first nozzle stage consists of a convergent-divergent nozzle with a contraction ratio of 19:1. This is designed so as to completely reflect the incident shock wave, thus producing a region of nearly stagnant air at high temperature and pressure behind the reflected shock. The divergent portion is contoured to produce uniform flow at about Mach 4. The second stage consists of a wedge-shaped plate placed at an angle of attack of 10° to the flow emerging from the first-stage nozzle. A Prandtl-Meyer expansion from the wedge deflects the air flow. Since the diaphragm particles, due to their higher momentum, cannot turn with the air stream, they are separated from the flow. The third stage is placed at 10° from the axis of the first stage to accept the centrifuged flow. This stage consists of a straight-walled, 15-degree included-angle nozzle terminating in an 11- by 15-inch test section. The test-section Mach number can be varied by changing the entrance area of the third-stage nozzle. All tests in the present investigation were conducted using one fixed area ratio.

Operational Procedure

Prior to shock tunnel operation, the test section is evacuated to approximately 1 micron of mercury. At the same time the driven and driver tubes are evacuated to prevent possible contamination of the charge gases. The driven tube is then pressurized with the gas chosen for the test (in these tests dry-air was used). Finally, the driver is pressurized with either hydrogen or helium to a pressure which permits the proper driver to driven pressure ratio for "tailored interface" operation[4].

Two methods of test initiation were used during this series. For the transverse-cylinder experiments, a single diaphragm was used between driver and driven tubes. After the driven pressure was set, the driver was pressurized until the diaphragm burst. The burst pressure of the metal diaphragm was controlled by the commonly-used technique of pressing an X in the diaphragm to a specific depth. At low pressures, when Mylar was used as the main diaphragm, the material strength was the determining factor for burst pressure. This practice gave burst pressure ratios which varied from run to run.

In order to obtain predictable and consistent burst pressures for the later hemisphere-cylinder tests, the double diaphragm technique* was tried. Two diaphragms of equal strength were placed between the driver and driven tubes such that a small volume of gas at about half the driver pressure could be held between them. The diaphragms were scribed so that they would, if used singly, burst at approximately 60 to 70 percent of the expected driver pressure. By pressurizing the region between the diaphragms to one-half the driver pressure and then loading the driver, the exact pressure ratio desired between driver and driven tubes could be obtained. To initiate the run, the pressure between the two diaphragms was reduced. This procedure was used successfully for driver pressures as low as 50 psig. Diaphragm burst pressures were extremely repeatable and could easily be varied.

*The first successful application of this technique brought to the authors' attention was by R. N. Cox of the A. R. D. E. at Fort Halstead, England. The first application at C. A. L. was in the 24" hypersonic shock tunnel operated by the Experimental Facilities Division.

Rupture of the diaphragm between the driver and driven tubes results in the formation of a shock wave which travels through the driven gas heating and compressing it. The shock wave reflects from the end of the driven tube and again passes through the test air further increasing the temperature and pressure. The resulting pressure causes the Mylar diaphragm between the driven tube, and nozzle to rupture, permitting the heated test air to pass through the three-stage hypersonic nozzle.

By utilizing the tailored-interface technique developed at C.A.L.[4], steady flow may be maintained in the test section for several milliseconds. With room-temperature helium as the driver gas, tailored-interface operation will produce stagnation temperatures in the range of 1800°K to 2000°K for a test duration of about 6-1/2 milliseconds. Using room-temperature hydrogen as the driver gas, stagnation temperatures from 3600°K to 4000°K are produced for flow periods of about 3-1/2 milliseconds.

Flow Conditions

The parameters recorded for each test are the following: initial gas pressure in the driven tube; driver gas pressure at the time the test is initiated; pressure behind the incident and reflected shock wave; incident shock wave speed; static pressure on the test section sidewall; the stagnation-point heat-transfer rate; the stagnation-point temperature change; test section pressure reading before vacuum system is closed; leak rate of test section; time from closing vacuum system to test initiation.

The pressure, temperature, enthalpy, and entropy of the air behind the reflected shock wave (which are the stagnation or reservoir conditions for the nozzle) are calculated from the measured shock speed and the initial air pressure using tables and charts for real air in thermodynamic equilibrium, for example, References 40-42. The agreement of the calculated and measured stagnation pressure provides a check as to the validity of the other calculated parameters. The test section Mach number is calculated using the measured free-stream static pressure and the stagnation pressure assuming isentropic flow in the nozzle. In most tests, the measured stagnation pressure and the value of stagnation pressure calculated using the incident

shock Mach number are not in agreement. Although the disagreement is appreciable, Figure 3, the effect on the reduced test-section conditions and data is not great. Figure 4 is a plot of the free-stream Mach number calculated using the static pressure and the stagnation or reservoir pressure both as measured and as calculated. Several possible reasons for the pressure difference exist. Inaccurate calibration of piezo-electric crystal transducers whose output signal is low at these pressure ranges does contribute some error. However, it is felt that this does not account for all of the error. The loss of mass flow through the convergent-divergent nozzle was studied to approximate that contribution. In the flow time in question there appeared to be little or no additional error. A small contribution is possible if shock attenuation is not accounted for between the final wave speed transducer and the end of the shock tube. This distance, however, is so small (5 inches) that even if attentuation were not considered here, the effect upon the value of the incident shock Mach number used in finding the stagnation pressure ratio would be negligible. One further possibility considered is that waves are initiated by diaphragm flaps which rebound from the driven tube walls after the diaphragm ruptures. This effect could vary depending upon the mass of the diaphragm flap. It would appear that any waves produced would have to lag behind the incident shock since no noticeable effect on wave speed has been witnessed.

Figure 3 indicates that a consistent difference in the measured and calculated pressures occurred both in the single-diaphragm and double-diaphragm tests. It is significant that the measured pressure was always less than the calculated pressure for the single-diaphragm runs and always greater for the double-diaphragm tests. This seems to indicate clearly that conditions at the diaphragm station are related to the discrepancy. Whether the difference is related to diaphragm opening time or by constriction of the flow by rebounding diaphragm flaps has not been determined. This matter requires further investigation. In any case, a consideration of the possible causes of the pressure difference seems to indicate that the measured pressure be used as the flow stagnation pressure.

This discrepancy between the measured and calculated pressures was only one of the difficulties encountered in making low pressure shock tunnel runs. In addition, there were such matters as increased shock wave attenuation (although it was still small enough to be unimportant), the difficulty in obtaining satisfactory low-pressure diaphragms (this was largely overcome by use of the double-diaphragm technique), and the thick nozzle-wall boundary layers (particularly in the first-stage nozzle which has a 1.5- by 12.25-inch exit cross-section). In spite of these problems, hypersonic low-density flow was obtained which was satisfactory for stagnation-point heat-transfer experiments.

As an indication of the degree of rarefaction which has been attained during this series of runs a curve of Knudsen number versus Reynolds number behind the shock wave, Re_s , has been plotted in Figure 5. In calculating the Knudsen number, the mean freepath, λ_s , behind the normal shock and body radius, R_b , have been used. The various rarefied flow regimes are indicated on this figure.

For the experiments in which helium was used as the driver gas, the range of flow conditions is given in Table I:

TABLE I
FLOW CONDITIONS FOR HELIUM DRIVER GAS EXPERIMENTS

RESERVOIR PRESSURE, p_0	2.4-58.0 ATM.
RESERVOIR TEMPERATURE, T_0	1500-2200 °K
FREE-STREAM VELOCITY, U_∞	5500-6700 FT/SEC
FREE-STREAM MACH NUMBER, M_∞	9.7-11.6
FREE-STREAM UNIT REYNOLDS NUMBER, Re_∞/L	1460-21,300 PER INCH
REYNOLDS NUMBER BEHIND SHOCK, Re_s	11-1000
KNUDSEN NUMBER, λ_s/R_b	0.036-.00048

For the tests using hydrogen as the driver gas, the range of flow conditions is listed in Table II:

TABLE II

FLOW CONDITIONS FOR HYDROGEN DRIVER GAS EXPERIMENTS

RESERVOIR PRESSURE, p_o	3.48-58.1 ATM.
RESERVOIR TEMPERATURE, T_o	3200-3700 °K
FREE-STREAM VELOCITY, U_∞	9000-10,000 FT/SEC
FREE-STREAM MACH NUMBER, M_∞	8.4-10.3
FREE-STREAM UNIT REYNOLDS NUMBER, Re_∞/L	561-3410 PER INCH
REYNOLDS NUMBER BEHIND SHOCK, Re_s	16-86
KNUDSEN NUMBER, λ_s/R_b	0.012-.002

Free-stream Mach number was calculated by isentropically expanding the stagnation conditions to the measured free-stream static pressure. A correction of the static pressure was made to account for the test section leak rate after the vacuum system was closed. The leak rate was noted and the time between closing of the vacuum system and rupture of the diaphragm was used to compute the back pressure on the static pressure transducer. A check upon this method of obtaining the free-stream Mach number was made using the results from a pitot probe placed in the air flow of the test region. The Mach number based on the ratio of pitot-to-reservoir pressures agreed with that calculated from the static pressure within the scatter of the results, Figure 4.

A certain amount of variation in reservoir temperatures can be seen in the tables (I and II). Obviously this variation also appears in the stagnation heat transfer, q . It results from the initial inconsistency of the pressure ratio at which the diaphragm between driver and driven tubes burst. Thus, a variation in shock Mach number occurs from run to run which produces a variation in temperature behind the reflected shock wave. Primarily, this inconsistency occurred during the transverse cylinder tests. The later hemisphere-cylinder tests utilized the double diaphragm technique which produced more repeatable flow conditions.

Tables I and II also indicate a variation of Reynolds number and free-stream Mach number. The variation of Mach number with Reynolds number

is caused by the influence of the nozzle-wall boundary layer. This is illustrated in Figure 4 which shows test section Mach number as a function of nozzle stagnation pressure.

Models and Instrumentation

Two series of shock tunnel tests have been mentioned previously. The first series included tests using three cylindrical models having nominal diameters of 1/8, 1/4, and 1 inch (Figure 6). The models were mounted transversely to the air stream with their axes in the plane of symmetry of the wedge-shaped final nozzle. Thin-film resistance thermometers[43] were mounted along the stagnation line of the cylinders. The 1/4-inch and 1-inch models had three resistance thermometers mounted about one inch apart. The 1/8-inch model had a single resistance thermometer.

For the second series a 1/2-inch diameter hemisphere-cylinder with a resistance thermometer mounted at the stagnation point of the hemispherical portion of the model was used, Figure 7. A technique described in References 43 and 44 was used whereby a resistance thermometer is formed by painting a 0.1 micron-thick platinum film upon a specified backing material, then curing the film by baking. The thin-film resistance thermometer was a rectangle measuring 1/16 inch either side of the stagnation point by approximately 1/32 inch wide. A colloidal-silver paint strip which is baked on the model acts as a lead to the wires at the rear of the hemisphere-cylinder. Resistance thermometers, when used for quantitative results, must be backed by a dielectric material with known, constant properties. Consequently, Pyrex glass was used in making all models tested in the two series. Since the heat capacity of the thin platinum film is negligible, it is assumed that the film temperature is the instantaneous surface temperature of the glass; thus heat lag due to film thickness may be neglected.

Calibration of the thin-film resistance thermometer is done using a controlled-temperature water bath. The model, enclosed in a watertight bag, is allowed to soak in the bath until it has reached the temperature of the bath. This is detected by a thermocouple on the model surface. As the bath temperature is increased, a linear rise in resistance is obtained. The normal calibration range is from room temperature to 50°C.

During a shock tunnel test the thermometers were operated at a constant electrical current so that surface temperature changes, which produced changes in film resistance, would result in a directly proportional voltage signal. This signal can be recorded directly on an oscillograph from which a temperature change can be obtained for later use in calculating the heat flux. The signal can also be fed into an analogue computer network such as described in Reference 45. The network converts the output of the thin-film resistance thermometer to an electrical signal proportional to the surface heat flux. An oscillograph record of heat-flux data is available immediately after a test run using the analogue network.

EXPERIMENTAL RESULTS

Transverse-Cylinder Tests

In the data reduction and presentation, the measured stagnation-point heat-transfer rate, q, has been nondimensionalized with respect to the quantity $\frac{1}{2}\rho_\infty U_\infty^3$. This is equivalent to the conventional Stanton number for the case of a cold wall, $T_w << T_0$. The data are presented in Figure 8 as the nondimensionalized heat transfer multiplied by the Reynolds number based on flow conditions behind the shock wave and body radius, $\frac{q\, Re_s}{\frac{1}{2}\rho_\infty U_\infty^3}$, and are plotted as a function of the Reynolds number behind the shock wave, Re_s.* The data represented by the open symbols are experiments for which the density ratio across the shock wave, $\epsilon \equiv \rho_\infty/\rho_s$, lies between 0.148 and 0.152; these are helium-driver-gas experiments for which the stagnation temperature is in the range from 1800°K to 2100°K. At the higher Reynolds numbers the data are seen to be in fairly good agreement with the boundary-layer theory of Fay and Riddell[26] as calculated for these flow conditions. At Reynolds numbers below 30 the data tend to fall increasingly below the boundary-layer theoretical prediction.

In the very low Reynolds number region of these experiments it was difficult to obtain precisely repeatable test conditions, because of the difficulty involved in making thin diaphragms that would burst at precisely the desired pressure.** Consequently, some of the data fall outside the density ratio range from 0.148 to 0.152, but rather were in the range from 0.157 to 0.163. These data are indicated by the half-filled symbols.

The hydrogen-driver-gas experiments are shown as the solid symbols, Figure 8. Only the 1/4-inch model has been tested at these conditions. For

---

* Utilizing the continuity equation across a normal shock wave, $\rho_\infty U_\infty = \rho_s U_s$, the Reynolds number behind the shock wave can be written as $Re_s = \frac{\rho_\infty U_\infty R_b}{\mu_s}$.

** Subsequent to these experiments, the double-diaphragm operating technique was introduced for the hemisphere-cylinder tests.

these experiments the density ratio was between 0.10 and 0.12 for stagnation temperatures from 3200°K to 3700°K. The boundary-layer theory has been calculated for a density ratio of 0.11. The data are seen to lie somewhat above the theory for this series of experiments, whereas for the lower stagnation temperature tests, the data fell below the theory in the same Reynolds number range. In view of the low stagnation pressure levels of these experiments, it was considered possible that the air flow might not be in thermodynamic equilibrium. The effects of freezing of the flow on the test-section conditions and on the stagnation-point heat-transfer rate have been investigated by Bray[46]. He has shown that freezing in the nozzle causes a reduction in the measured heat-transfer rate. At temperatures of 3700°K and less, nonequilibrium effects would be expected to be small. The agreement of the present data with theory indeed indicates that these effects were apparently negligible, and the assumption that the flow is in equilibrium is reasonably accurate.

It is observed in Figure 8 that the low stagnation temperature data (open and half-filled symbols) tend to lie below the boundary-layer theory for all Reynolds numbers below 30, whereas the high-temperature data (solid symbols) are in good agreement with theory at Reynolds numbers down to 16. This results from the difference in the degree of rarefaction of the two flows at a given Reynolds number. For example, at a Reynolds number of 20, the low-temperature flow has a Knudsen number of 0.02, while the high-temperature flow has a Knudsen number of only 0.01. Hence, the one flow is almost twice as rarefied as the other at a given Reynolds number.

For the sake of comparison at the lowest Reynolds numbers, heat-transfer rates have been calculated according to classical free-molecule theory[12]. These are shown for accommodation coefficients of 1, 1/2, and 1/4 (Figure 8). Although the lower stagnation temperature data (open and half-filled symbols) appear to tend toward agreement with free-molecule theory for an accommodation coefficient of about 1/4, it would be erroneous to conclude that the data indicate an accommodation coefficient substantially below unity. Even for the lowest Reynolds number experiments, the Knudsen

number, which is about 0.02, is about two orders of magnitude below that of free-molecule flow, $Kn > 1$. At the lowest Reynolds numbers (Figure 5), the flow is in the fully-merged region as described in References 6, 12 and 18. It should be noted that in the region of Knudsen numbers above 0.01, the use of the inviscid Rankine-Hugoniot equations to calculate flow conditions behind the shock wave is highly questionable.

The various symbols (○△□) used in Figure 8 indicate the three heat-transfer gauges spaced about 1 inch apart along the span of the 1/4- and 1-inch diameter models, Figure 6. The purpose of the three gauges was to check the spanwise flow uniformity. No systematic variation greater than the data scatter can be detected in Figure 8.

Presentation of stagnation-point heat transfer in the form of Figure 8 shows a great sensitivity to the density ratio, $\epsilon = \rho_\infty/\rho_s$. The recent work by Cheng[13] has shown that much of this sensitivity can be removed by presenting the information in the form of Figure 9. Here the stagnation-point heat transfer is presented as the heat-transfer coefficient

$$C_H = \frac{q}{\rho_\infty U_\infty (H_0 - H_w)} \qquad (1)$$

plotted versus the product of the density ratio and the Reynolds number behind the shock, ϵRe_s. Note that the high stagnation temperature data (solid symbols) and the low-temperature data (open symbols) and the corresponding boundary-layer theories are in close agreement when presented in this manner. As before, this presentation does not reveal the difference in degree of rarefaction of the flow for these two series of experiments. Hence, the low-temperature data tend to depart from the boundary-layer theory below values of ϵRe_s of 4, whereas the high-temperature data are still in good agreement with this theory at $\epsilon Re_s = 2$.

Hemisphere-Cylinder Tests

The stagnation-point heat-transfer data for the hemisphere-cylinder experiments* is presented in Figure 10. The heat-transfer rate q is plotted

*These tests were supported by the U. S. Navy Office of Naval Research under Contract Nonr-2653(00).

as the heat transfer parameter, C_H , versus the parameter Λ , which results from Cheng's analysis and is given by

$$\Lambda = \frac{\frac{2}{3} Pr}{\sqrt{1 + \frac{4}{K^2}} - 1} \tag{2}$$

where

$$K^2 = \frac{\rho_\infty R_b}{\mu_\infty U_\infty C} = \epsilon' Re_s \left(\frac{\mu_0}{\mu_*} \frac{T_*}{T_0} \right) \tag{3}$$

T_* is a reference temperature obtained from the analysis. For the present test conditions, the corresponding values of K^2 and $\epsilon' Re_s$ are indicated along the abscissa of Figure 10. For strong shock waves where $\rho_\infty << \rho_s$ and $U_s << U_\infty$, the parameter $\epsilon' = \frac{\rho_s}{2\rho_s H_s}$ and the density ratio across the shock wave, $\epsilon = \rho_\infty / \rho_s$, are essentially identical. However, at conditions of the present experiments these parameters differ slightly. For example, in a typical case, $\epsilon = \rho_\infty / \rho_s = 0.15$ where $\epsilon' = \frac{\rho_s}{2\rho_s H_s} = 0.12$.

The theoretical curves shown in Figure 10 represent; (1) a complete numerical solution of the viscous shock-layer equations by Cheng for $\epsilon' = 0.10$ and 0.15, (2) Cheng's analytic solution for the fully viscous flow, (3) Cheng's numerical boundary-layer solution including vorticity (this is coincident with the complete numerical solution*) for $\epsilon' = 0.10$ and 0.15, and (4) the boundary-layer theory of Fay and Riddell[26] which does not include vorticity effects. The analytic solution of the fully viscous flow is a zero-order result. Higher order solutions can be obtained from Cheng's analysis[13] which will exhibit closer agreement with the numerical solution at higher values of the parameter, Λ.

---

*The boundary-layer solution differs from the complete numerical solution in that the boundary-layer approximations are employed to drop some terms in the Navier-Stokes equations. The two results are essentially identical numerically at $\Lambda > 5$.

The data are seen to be in fairly good agreement with the theory, although the scatter is greater at the lower Reynolds number, Figure 10. Although these experiments extend over a rather limited range (only about one and a half orders of magnitude in Knudsen number or Reynolds number), they cover an important region from the vorticity-interaction regime through the incipient merged-layer regime, Figure 5. It is noted that even at the highest Reynolds number of these experiments, the vorticity-interaction effect amounts to a 10 percent increase in heat transfer.

Both the present data and some of the data of Ferri et al[10] are compared with Cheng's theory in Figure 11. The theoretical curves have been calculated for values of ϵ' of 0.10 and 0.15, a Prandtl number of 0.71 and a wall-to-stagnation temperature ratio, T_w/T_o, of zero. These values of ϵ' bracket the experimental data which fall in the range $0.120 \leq \epsilon' \leq 0.131$. The wall-to-stagnation temperature ratios for the experiments ranged from 0.150 to 0.175 for the C.A.L. experiments and had values of 0.34 and 0.46 for the PIBAL experiments*. Ferri's data is seen to have less scatter and to be in better agreement with the theory than the present data.

It should be indicated, that the PIBAL data is presented in Reference 10 only as the ratio of measured heat-transfer rate with vorticity interaction to measured heat-transfer rate without voticity interaction. This results from the experimental technique which consists of testing simultaneously several models of different radii at very high Reynolds numbers, where the vorticity interaction should be zero, and using the value of $q\sqrt{R_b}$ obtained in these experiments as the zero-vorticity reference. The fact that $q\sqrt{R_b}$ does not change from model to model verifies that the vorticity interaction was zero for these experiments. Then the various sized models were tested at a range of Reynolds numbers, and the ratio of the quantity $q\sqrt{R_b}$ for each model to the value of $q\sqrt{R_b}$ for the largest model is determined. This is taken as the ratio of heat transfer with vorticity to heat transfer without vorticity after

---

*These values are inferred from the fact that the theory in Reference 10 is calculated for values of H_w/H_o of 0.34 and 0.46 (see Figure 4, Reference 10). For the flows conditions of Reference 10, T_w/T_o can be taken equal to H_w/H_o.

the value of $q\sqrt{R_b}$ for the largest model is corrected for vorticity interaction by ratioing to the value obtained from the high Reynolds number tests, and the ratio of the model radii is evaluated. Thus, Ferri et al[10] present the data as $q_{vort}/q_{vort=0}$ as a function of Reynolds number, $Re = \rho_{os}\sqrt{H_{os}}\,R_b/\mu_{os}$, where q_{vort} is the measured heat-transfer rate. The quantity $q_{vort=0}$ was determined by reducing the heat-transfer rate measured on the largest model of the test by the square root of the ratio of the radii and by the ratio of the heat-transfer rate for the largest model to the heat-transfer rate to this model for the high Reynolds number test.

This technique is used to eliminate or reduce random and systematic errors occurring in the measurement of the flow conditions and in the model instrumentation. The use of this technique accounts for the smaller scatter of the PIBAL data relative to the C.A.L. data. As has been indicated, the present data is reduced directly from the measured heat-transfer rate and the measured and calculated flow conditions. To compare the two sets of data with Cheng's theory in terms of absolute values of heat-transfer coefficient, a zero-vorticity heat-transfer rate has been calculated for the PIBAL test conditions using the theory of Fay and Riddell[26]. The details are given in the Appendix.

Considering the degree to which the test flow conditions differ from the assumptions of the theory (e.g., $T_w/T_0 = 0.46$ for the PIBAL experiments and $T_w/T_0 = 0$ for the theory), the agreement over such a wide range of Reynolds numbers is remarkably good. Furthermore, the theory shows, Figure 11, that data obtained at different flow conditions can be correlated in terms of parameters such as λ, K^2 or $\epsilon' Re_s$.

FUTURE SHOCK TUNNEL DEVELOPMENT AND LOW-DENSITY RESEARCH

The present experiments have demonstrated the application of the shock tunnel to hypersonic, rarefied-gasdynamic research. To determine the over-all suitability of the shock tunnel in this research field, a thorough investigation has been made of the requirements for a hypersonic, low-density wind tunnel. This study has considered instrumentation, simulation requirements, and shock tunnel capabilities. A brief review of these items will be given here.

Instrumentation Developments

Quite naturally one of the first matters of concern is the instrumentation, since it is of little value to produce a hypersonic rarefied-gas flow if no measurements can be made. The present heat-transfer instrumentation will sense heat-transfer rates of less than 1 B.T.U./sq ft/sec. This is sufficient to measure the heat transfer about one foot from the nose of a slender cone at a density altitude of 200,000 ft at Mach 5 and 325,000 ft at Mach 20. Thus, no additional development of heat-transfer instrumentation is needed for experiments within this flight envelope.

The pressure transducers now in use have sensitivities sufficient to measure a static pressure of 4×10^{-5} atm which corresponds to an altitude of 330,000 ft. These transducers are modified Altec-Lansing microphones, Type 21BR-180-2, which are of the variable capacitance type. In addition, small-size piezoelectric transducers having comparable sensitivity and a much lower acceleration sensitivity are currently being developed at CAL[5].

Present force-sensing instrumentation is highly refined as are the heat transfer and pressure techniques and is adequate for measuring lift, drag, and pitching moment on blunt bodies. Further improvements can be expected to provide sufficient sensitivity to extend these measurements to slender bodies. The free-flight technique reported in References 47 and 48 can also be used. Thus, instrumentation techniques are available for making

heat transfer, pressure and force measurements in hypersonic, rarefied air flow in a shock tunnel.

Simulation Requirements

Next, consideration has been given to the flow quantities and parameters that must be either duplicated or simulated in a low-density, hypersonic wind tunnel. Among the more obvious of these are Mach number, Reynolds number, Knudsen number, shock-wave density ratio, and specific-heat ratio. Each experiment requires some analysis of the flow phenomena to determine the important parameters or conditions requiring duplication. In general, however, a hypersonic, low-density wind tunnel should be capable of simultaneously achieving both high Mach numbers and hypervelocities over a wide range of Reynolds numbers. Again, the shock tunnel has a proven capability in this respect. The subject of simulation requirements and shock tunnel capabilities is covered in more thorough detail in References 5 and 49.

Two very important phenomena that may be encountered in hypersonic, low-density wind tunnels are thermodynamic nonequilibrium (or relaxation effects) in the nozzle flow[46] and thick nozzle-wall boundary layers. Nonequilibrium effects can be avoided by restricting the stagnation temperature to values below which vibration, dissociation, ionization and nitric-oxide formation occur. This, however, directly limits the flow velocity to values of 7000 ft/sec or less. The attainment of higher speeds requires stagnation temperatures of 2000°K or greater. At high stagnation temperatures, nonequilibrium effects can become very significant, particularly if low stagnation pressures are used. It appears necessary, therefore, when operating at high stagnation temperatures, also to operate at high stagnation pressures to minimize nonequilibrium effects[50]. Low Reynolds numbers are then obtained naturally from the expansion of the flow to very high Mach numbers and low pressures and temperatures. This is precisely the technique that must be used to duplicate flight conditions as has been indicated in References 5 and 49. The shock tunnel is extremely well-suited for this type of operation, and its short test duration is a distinct advantage for high stagnation pressure and temperature operation.

It is well known that the nozzle-wall boundary-layer thickens as the stagnation pressure, and hence free-stream Reynolds number, is decreased. Boundary-layer thickness also increases strongly with Mach number[51]. Consequently, hypersonic wind tunnels are generally so plagued by such thick boundary layers that in many cases only a small core of good flow exists along the nozzle centerline. In view of this characteristic, it seems desirable that low-density, hypersonic nozzles be relatively large, say on the order of several feet or greater in diameter. Nozzles of this size would require a very large vacuum pumping system, if they were to operate continuously. Here, the shock tunnel possesses a favorable feature in its intermittent operation because extremely high-capacity pumping systems are not required.

Shock Tunnel Developments

These considerations of the requirements of a hypersonic, low-density wind tunnel have led to the conclusion that the shock tunnel possesses many features which make it well-suited for rarefied-gasdynamic research. It should be mentioned, however, that the foregoing discussion is primarily intended to bring attention to the advantages of the shock tunnel and is not meant to imply that it is the only facility suitable for research in hypersonic, rarefied gasdynamics.

In view of the apparent advantages possessed by the shock tunnel as a hypersonic, low-density facility, CAL has undertaken construction of a shock tunnel having a large-scale nozzle capable of expanding the air from high stagnation pressures and temperatures to high Mach numbers over a wide range of Reynolds numbers. This tunnel will have a 6-foot diameter test section and will operate at stagnation temperatures up to 8000°K and stagnation pressures up to 2000 atm. These conditions will permit the attainment of hypervelocity low-density flow with minimized nonequilibrium effects. The Mach number range will be from about 15 to 25, and the test flow duration will be about 5 milliseconds. Based upon the success attained during the present experiments utilizing a shock tunnel that was never designed for low-density operation, the new 6-foot shock tunnel should prove to be an extremely useful tool for research in hypersonic, rarefied gasdynamics.

SUMMARY

The experimental results presented here have shown that, for a two-dimensional stagnation point (transverse cylinder), the boundary-layer theory of Fay and Riddell predicts the heat transfer very well even when the flow behind the shock wave is fully viscous. No increase in heat transfer due to viscous-layer effects could be detected on the transverse cylinder.

The results of tests of an axisymmetric stagnation point (hemisphere cylinder) indicate that vorticity-interaction and viscous-layer effects increase the heat transfer significantly above that predicted by boundary-layer theory. A new theory by H. K. Cheng at CAL has been used to correlate the hemisphere data. The agreement is quite good over the entire range of the data which extends from the vorticity-interaction regime through the incipient merged layer regime.

It is clear that additional experiments at lower Reynolds numbers (higher Knudsen numbers) are needed to establish the transition from continuum to free-molecule theory. The new 6-foot shock tunnel now under construction at CAL should permit extension of the range of the experiments to the free-molecule flow regime.

REFERENCES

1. Stalder, J.R., The Use of Low-Density Wind Tunnels in Aerodynamic Research, Paper presented at the 1st Internat'l. Symp. on Rarefied Gas Dynamics, Nice, France, July 1958 (Published in the proceedings of the Symposium "Rarefied Gas Dynamics," Edit. by F.M. Devienne, Pergamon Press, New York, 1959.)

2. Drake, R.M. and Backer, G.H., Heat Transfer from Spheres in Supersonic Flow to a Rarefied Gas, Trans. ASME, Vol. 74, October 1952.

3. Schaaf, S.A., Aerodynamics at Very High Altitudes, Jet Propulsion, Vol. 26, No. 4, pp 247-250, April 1956.

4. Wittliff, C.E., Wilson, M.R., and Hertzberg, A., The Tailored-Interface Hypersonic Shock Tunnel, CAL Report No. AD-1052-A-8, AFOSR TN 59-31, AD 209203 (Jan. 1959); Also J. Aero/Space Sci., Vol. 26, No. 4, April 1959.

5. Hertzberg, A. and Wittliff, C. E., Studying Hypersonic Flight in the Shock Tunnel, I.A.S. Paper No. 60-67 presented at the Nat'l Summer Meeting, Los Angeles, Calif., June 1960.

6. Probstein, R.F. and Kemp, N.H., Viscous Aerodynamic Characteristics in Hypersonic Rarefied Gas Flow, J.A./S.S., Vol. 27, No. 3, pp 174-192, March 1960.

7. Herring, T.K., The Boundary Layer Near the Stagnation Point in Hypersonic Flow Past a Sphere, J. Fluid Mech., Vol. 7, Part 2, pp 257-272, February 1960.

8. Hoshizaki, H., Shock-Generated Vorticity Effects at Low Reynolds Numbers, Lockheed M.S.D. Rept. LMSD-48381, Vol. 1, pp 9-43, January 1959.

9. Ho, H.T. and Probstein, R.F., The Compressible Viscous Layer in Rarefied Hypersonic Flow, Brown Univ., ARL TN 60-132, August 1960.

10. Ferri, A., Zakkay, V. and Ting, L., Blunt Body Heat Transfer at Hypersonic Speed and Low Reynolds Numbers, PIBAL Rept. No. 611 (ARL TN 60-140), June 1960.

11. Wittliff, C.E. and Wilson, M.R., Low-Density Research in the Hypersonic Shock Tunnel, Paper presented at the 2nd Internat'l. Symp. on Rarefied Gas Dyn., Univ. of Calif., Berkely, Calif., August 3-6, 1960.

12. Hayes, W.D. and Probstein, R.F., "Hypersonic Flow Theory," Academic Press, New York, 1959.

13. Cheng, H.K., Aerodynamic Study of Shock-Detachment Zone at Moderate Reynolds Number, C.A.L. Memo for the Record, October 1960.

14. Tsien, H.S., Superaerodynamics, Mechanics of Rarefied Gases, J.A.S., Vol. 13, No. 12, pp 653-664, December 1946.

15. Probstein, R.F., Continuum Theory and Rarefied Hypersonic Aerodynamics, Brown Univ., WADC TN 58-145, July 1958 (also F.M. Devienne, Edit., "Rarefied Gas Dynamics," pp 418-433, Pergamon Press, New York, 1960.)

16. Probstein, R.F., Aerodynamics of Rarefied Gases, Brown Univ., WADC TN 58-228, July 1958 (also F.M. Devienne, Edit., "Rarefied Gas Dynamics," pp 262-279, Pergamon Press, New York, 1960.)

17. Oguchi, H., Hypersonic Flow Near the Forward Stagnation Point of a Blunt Body of Revolution, J.A./S.S., Vol. 25, No. 12, pp 789-790, December 1958.

18. Probstein, R.F., Shock Wave and Flow Field Development in Hypersonic Re-entry, Amer. Rock. Soc., Paper 1110-60 presented at ARS Semi-Annual Meeting, Los Angeles, Calif., May 1960.

19. Tewfik, O.K. and Giedt, W.H., Heat Transfer, Recovery Factor, and Pressure Distributions Around a Circular Cylinder Normal to a Supersonic Rarefied-Air Stream, J.A./S.S., Vol. 27, No. 10, pp 721-729, October 1960.

20. Weltmann, R.N. and Kuhns, P.W., Heat Transfer to Cylinders in Crossflow in Hypersonic Rarefied Gas Streams, NASA TN D-267, March 1960.

21. Hoshizaki, H., Neice, S. and Chan, K.K., Stagnation Point Heat Transfer Rates at Low Reynolds Numbers, I.A.S. Paper No. 60-68 presented at the Nat'l. Summer Meeting, Los Angeles, Calif., June 1960.

22. Varwig, R.L., Measurements of Free Molecule Heat Transfer in Air at Mach Numbers from 10-18, Space Tech. Lab. Rept. No. STL/TR-60-0000-94324, October 1960.

23. Sibulkin, M., Heat Transfer Near the Forward Stagnation Point of a Body of Revolution, J.A.S., Vol. 19, No. 8, pp 570-571, August 1952.

24. Reshotko, E. and Cohen, C.B., Heat Transfer at the Forward Stagnation Point of Blunt Bodies, NACA TN 3513, July 1955.

25. Lees, L., Laminar Heat Transfer Over Blunt-Nosed Bodies at Hypersonic Flight Speeds, Jet Propulsion, Vol. 26, No. 4, pp 259-269, April 1956.

26. Fay, J.A. and Riddell, F.R., Theory of Stagnation Point Heat Transfer in Dissociated Air, J.A.S., Vol. 25, No. 2, pp 73-85, February 1958.

27. Goldstein, S., Edit., "Modern Developments in Fluid Dynamics," Vol. 2, p. 631, Oxford Univ. Press, London, 1938.

28. Oguchi, H., The Blunt Body Viscous Layer Problem With and Without an Applied Magnetic Field, Brown Univ., WADD TN 60-57, February 1960 (also Phys. of Fluids, Vol. 3, No. 4, pp 567-580, July-August 1960).

29. Lunc, M. and Lubonski, J., Sur Une Solution Approchee' du Probleme de L'e'coulement d'un Gaz Rare'fie' Autour d'un Obstacle, Arch. Mech. Stos., Vol. 8, pp 597-616, 1956.

30. Baker, R.M.L., Jr. and Charwat, A.F., Transitional Correction to the Drag of a Sphere in Free-Molecule Flow, Phys. of Fluids, Vol. 1, No. 2, pp 73-81, March-April 1958.

31. Hammerling, P. and Kivel, B., Heat Transfer to a Sphere at the Transition from Free-Molecule Flow, Phys. of Fluids, Vol. 1, No. 4, pp 357-358, July-August 1958.

32. Liu, V.C., On Pitot Pressure in an Almost-Free-Molecule Flow-A Physical Theory for Rarefied-Gas Flows, J.A./S.S., Vol. 25, No. 12, pp 779-785, December 1958.

33. Willis, D.R., On the Flow of Gases Under Nearly Free Molecular Conditions, Princeton Univ., Dept. Aero. Eng., Rept. No. 442, 1958.

34. Schaaf, S.A. and Chambre', P.L., "Fundamentals of Gas Dynamics," Sec. H., Flow of Rarefied Gases, pp 687-736, Princeton Univ. Press, Princeton, N.J., 1958.

35. Schaaf, S.A. and Talbot, L., Handbook of Supersonic Aerodynamics, Sec. 16, Mechanics of Rarefied Gases, NAVORD Rept. 1488 (Vol. 5), February 1959.

36. Chapman, D.R. and Rubesin, M.W., Temperature and Velocity Profiles in the Compressible Laminar Boundary Layer with Arbitary Distribution of Surface Temperature, J.A.S., Vol. 16, No. 9, pp 547-565, September 1949.

37. Freeman, N.C., On the Theory of Hypersonic Flow Past Plane and Axially-Symmetric Bluff Bodies, J. Fluid Mech., Vol. 1, pp 366-387, October 1956.

38. Chester, W., Supersonic Flow Past a Bluff Body with a Detached Shock, Part II, Axisymmetric Body, J. Fluid Mech., Vol. 1, pp 490-496, November 1956.

39. Glick, H.S., Hertzberg, A., and Smith, W.E., Flow Phenomena in Starting a Hypersonic Shock Tunnel, CAL Rept. No. AD-789-A-3, AEDC-TN-55-16, AD 56231, March 1955.

40. Moeckel, W.E. and Weston, K.C., Composition and Thermodynamic Properties of Air in Chemical Equilibrium, NACA TN 4265, April 1958.

41. Hilsenrath, J., Klein, M., and Wooley, H.W., Tables of Thermodynamic Properties of Air Including Dissociation and Ionization from 1500°K to 15,000°K, Nat'l. Bur. Std., AEDC TR 59-20, December 1959.

42. Erickson, W.D. and Creekmore, H.S., A Study of Equilibrium Real-Gas Effects in Hypersonic Air Nozzles, Including Charts of Thermodynamic Properties of Equilibrium Air, NASA TN D-231, April 1960.

43. Vidal, R.J., Model Instrumentation Techniques for Heat Transfer and Force Measurements in a Hypersonic Shock Tunnel, CAL Rept. No. AD-917-A-1, PB 138852, WADC TN 56-315, AD 97238, February 1956.

44. Wittliff, C.E. and Rudinger, G., Summary of Instrumentation Development and Aerodynamic Research in a Hypersonic Shock Tunnel, CAL Rept. No. AD-917-A-2, Part I, PB 151488, WADC TR 58-401, AD 155758, August 1958.

45. Skinner, G.T., Analog Network to Convert Surface Temperature to Heat Flux, CAL Rept. No. CAL-100, February 1960.

46. Bray, K.N.C., Atomic Recombination in a Hypersonic Wind Tunnel Nozzle, J. Fluid Mech., Vol. 6, Part 1, pp 1-32, January 1959.

47. Naval Ordnance Laboratory Aeroballistic Research Facilities, Nav. Ord. Rept. No. NOLR 1233, 1959.

48. Geiger, R.E., Experimental Lift and Drag of a Series of Glide Configurations at Mach Numbers 12.4 and 17.5, I.A.S. Paper No. 60-92 presented at the Nat'l. Summer Meeting, Los Angeles, Calif., June 1960.

49. Wittliff, C.E., Hypersonic Research in the Shock Tunnel, Paper presented at the I.A.S. National Symposium on Hypervelocity Techniques, Denver, Colo., October 20,21, 1960.

50. Hall, J.G. and Russo, A.L., Studies of Chemical Nonequilibrium in Hypersonic Nozzle Flows, C.A.L. Rept. No. AD-1118-A-6 (AFOSR TN 59-1090), November 1949.

51. Lee, J.D., Axisymmetric Nozzles for Hypersonic Flows, Ohio State Univ. Rept. No. TN (ALOSU) 459-1 (WADC TN 59-228), June 1958.

APPENDIX

The procedure used to convert the PIBAL data from the form of presentation in Reference 10 to the present form, Figure 11, is described in this Appendix. The approximations and assumptions involved are indicated.

The experimental data are presented by Ferri et al[10] as the ratio $q_{vort}/q_{vort=0}$ versus Reynolds number. The quantity q_{vort} is the measured heat-transfer rate. The quantity $q_{vort=0}$ was determined experimentally from the largest diameter model for which the vorticity effects are zero and the square root of the ratio of the radii of the models. The Reynolds number is defined as*

$$Re_{os} = \frac{\rho_{os}\sqrt{H_{os}}\,R_b}{\mu_{os}} \qquad \text{(A1)}$$

where the quantities ρ_{os}, H_{os} and μ_{os} are the density, enthalpy and viscosity, respectively, evaluated at stagnation-point conditions behind the bow shock. R_b is the body radius.

The experimental conditions are free-stream Mach number of 8 and stagnation temperatures of 890°K (1600°R) and 1280°K (2300°R). The range of stagnation pressures is not specified; however, they can be determined from the quoted values of Reynolds number. The ratio of wall-to-stagnation enthalpies is taken as 0.46 and 0.34 for the 890°K and 1280°K experiments, respectively.

The Reynolds number of Reference 10, Re_{os}, is related to the Reynolds number behind the shock of the present experiments and Cheng's theory, $Re_s = \frac{\rho_\infty U_\infty R_b}{\mu_s}$, as follows

$$Re_s = \epsilon\sqrt{2\,(1 - H_\infty/H_0)}\left(\frac{\rho_s}{\rho_{os}}\right) Re_{os} \qquad \text{(A2)}$$

*The notation of the present report rather than Reference 10 is used here.

where $\epsilon = \rho_\infty/\rho_s$, $H_o = H_{os}$ and μ_s has been taken equal to μ_{os} which is a good approximation at these flow conditions.

To express the PIBAL data given as $q_{vort}/q_{vort=0}$ versus $Re_{os} = \frac{\rho_{os} R_b \sqrt{H_{os}}}{\mu_{os}}$ in terms of $C_H = q/\rho_\infty U_\infty (H_o - H_w)$ and $k = \frac{2}{3} Pr/\left(\sqrt{1+4/K^2} - 1\right)$ where $K^2 = \epsilon' Re_s \left(\frac{\mu_{os}}{\mu_*} \frac{T_*}{T_{os}}\right)$, the procedure is as follows:

(1) Re_s is calculated from Eq. (A2)

(2) k is calculated from Eqs. (2) and (3)

(3) $C_{H\,vort\,=\,0}$ is calculated using the theory of Fay and Riddell[23]

(4) C_H is taken as $\left(\frac{q_{vort}}{q_{vort=0}}\right) C_{H\,vort\,=\,0}$

The PIBAL data plotted in Figure 11 have been obtained in this manner. It has been necessary to assume $M_\infty = 8$ and $T_o = 890°K$ and $1280°K$ exactly for all the data because the variation of M_∞ with Reynolds number and the repeatability of T_o for different tests are not given.

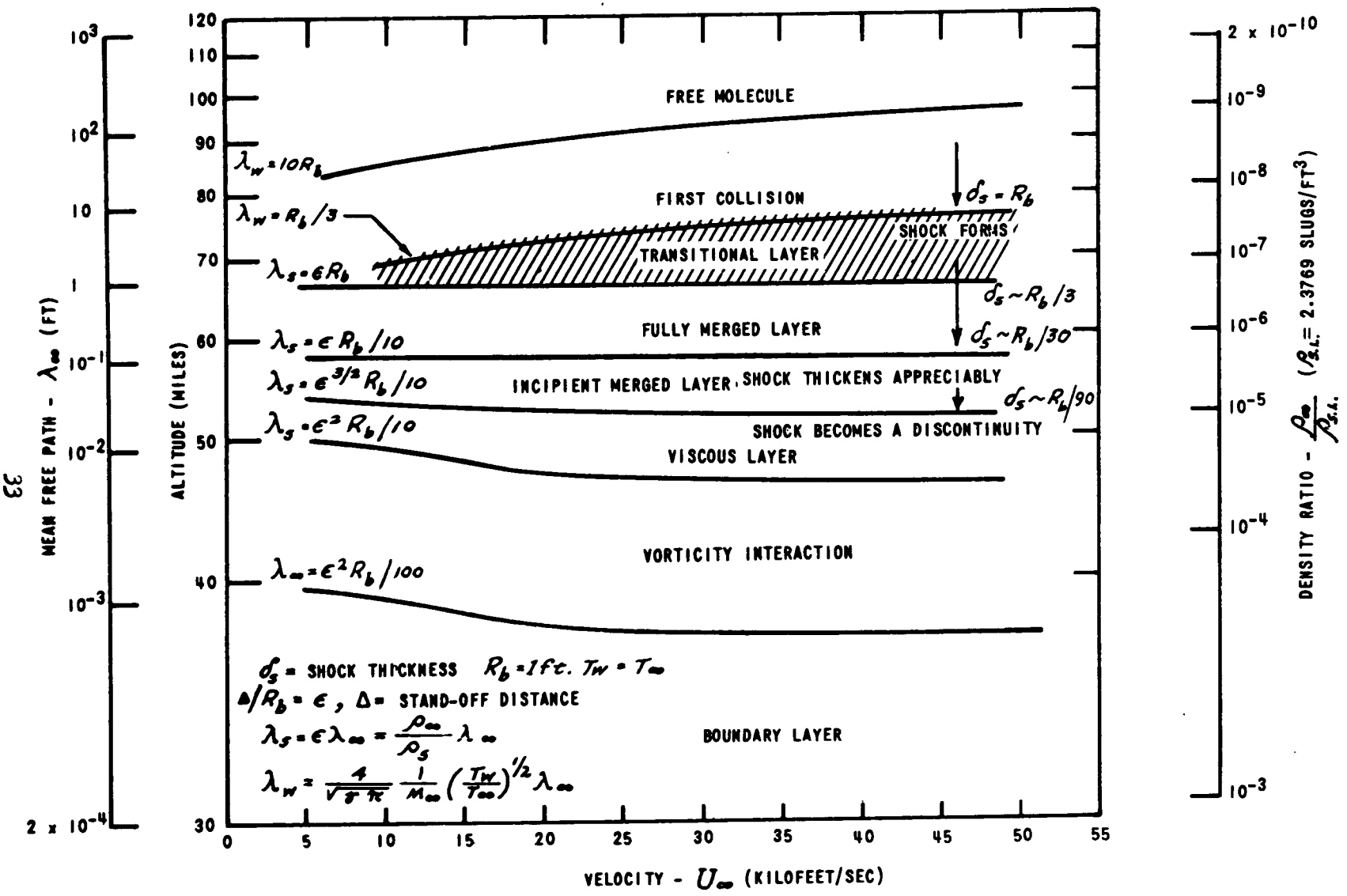

Figure 1 RAREFIED GAS FLOW REGIMES FOR STAGNATION REGION OF A HIGHLY COOLED BLUNT BODY FLYING AT HYPERSONIC SPEEDS (ADAPTED FROM REF. 18)

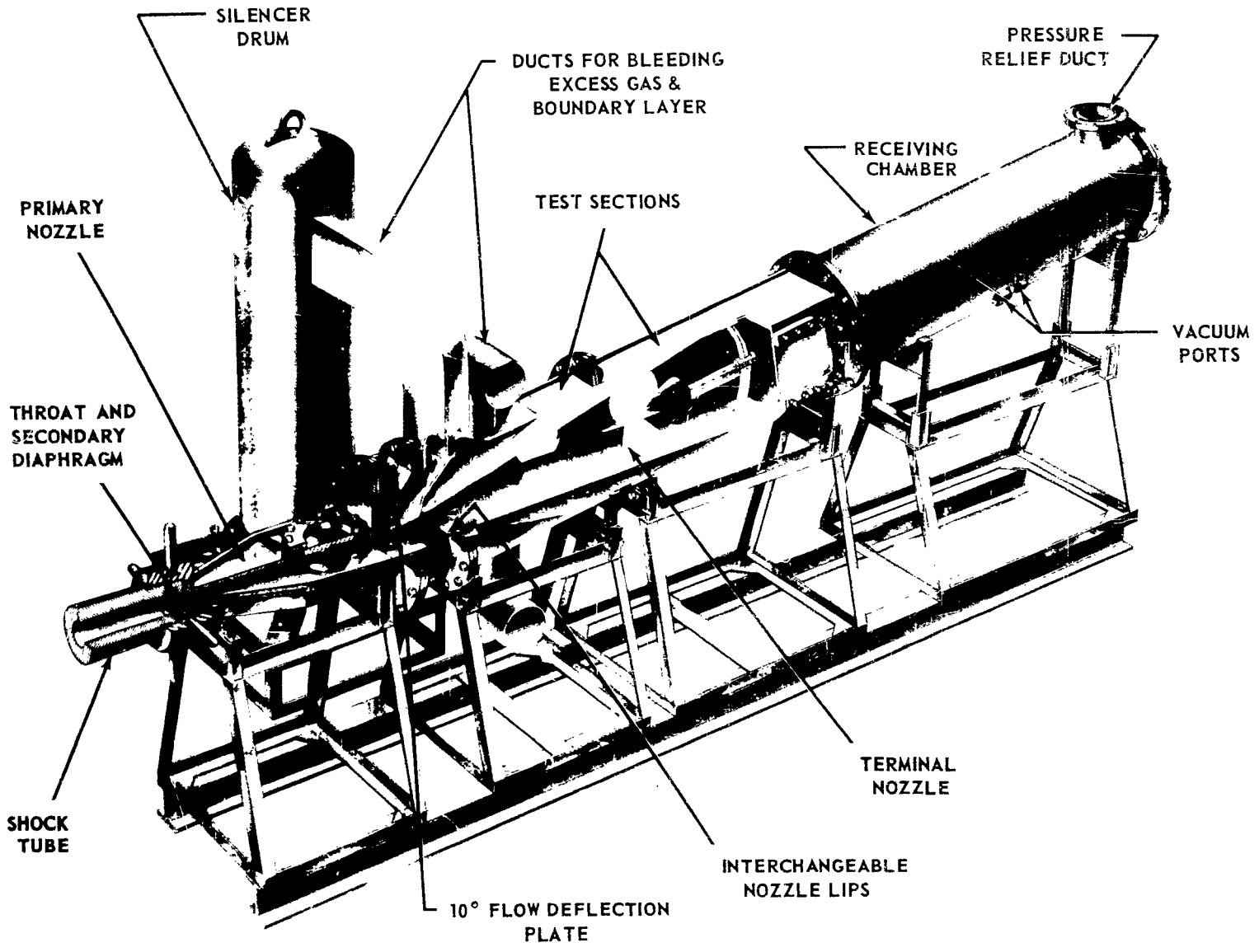

Figure 2 11 x 15 INCH CAL HYPERSONIC SHOCK TUNNEL

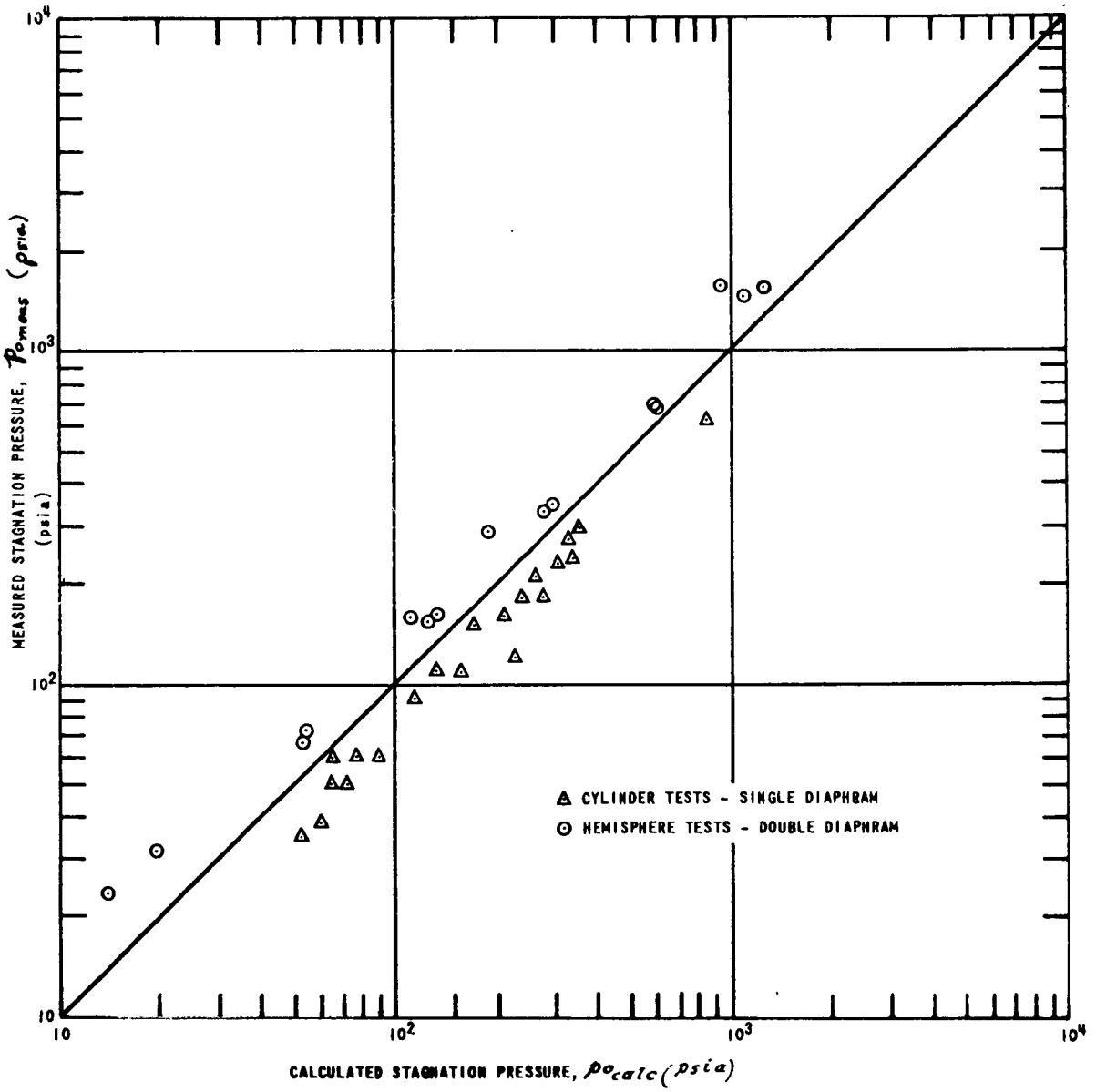

Figure 3 CORRELATION OF MEASURED AND CALCULATED STAGNATION PRESSURES

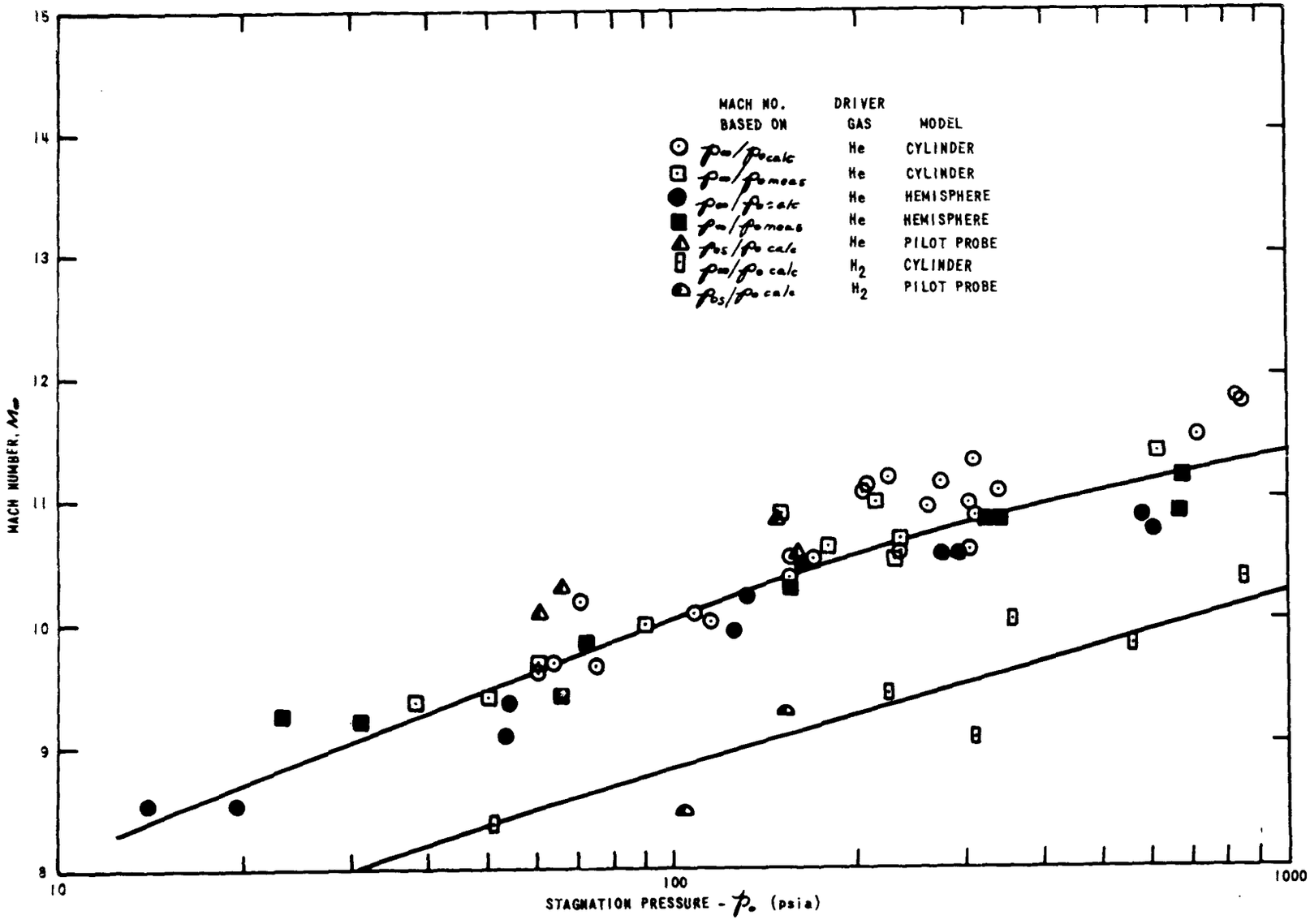

Figure 4 MACH NUMBER VARIATION WITH NOZZLE STAGNATION PRESSURE

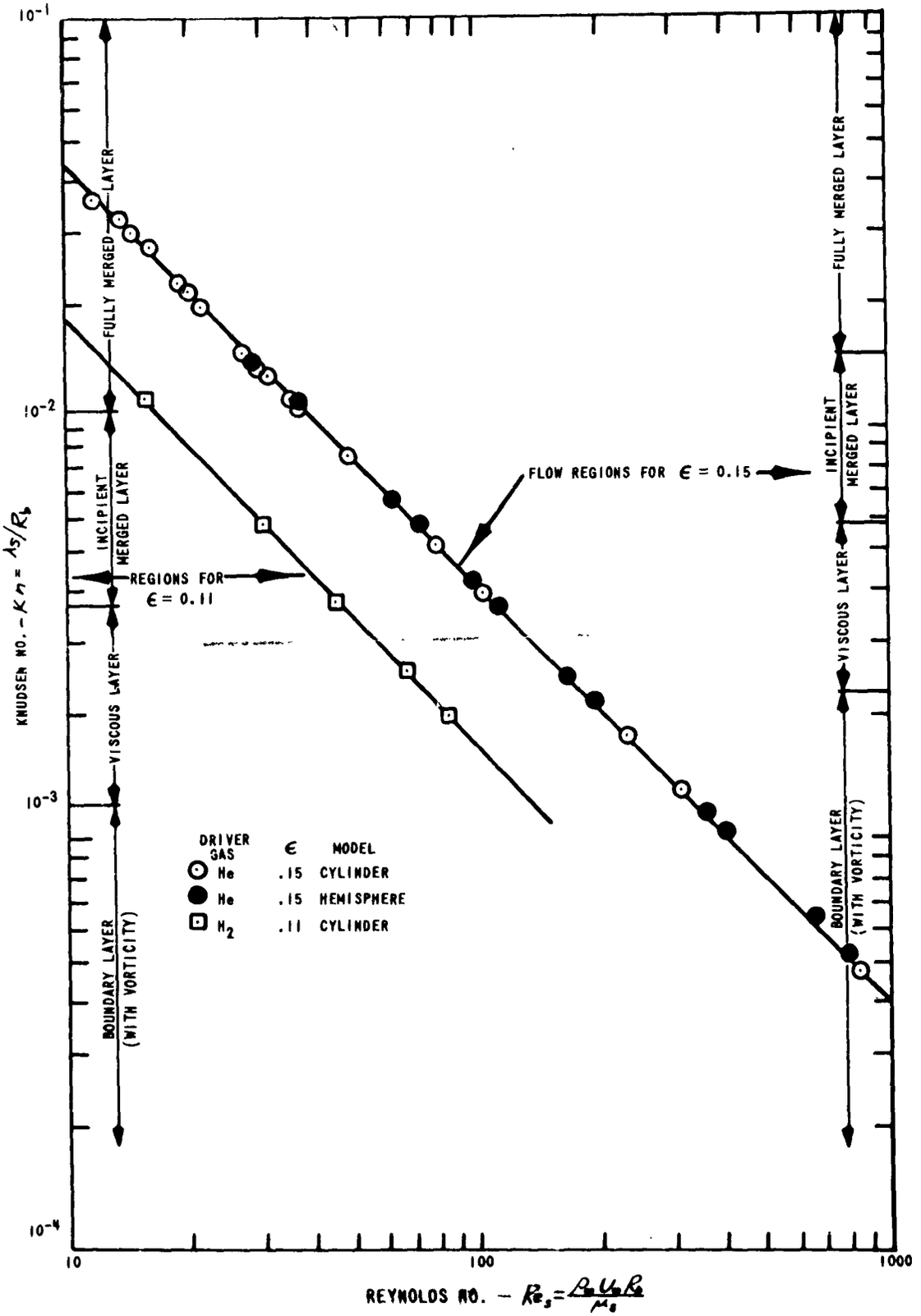

Figure 5 KNUDSEN NUMBER VARIATION WITH REYNOLDS NUMBER

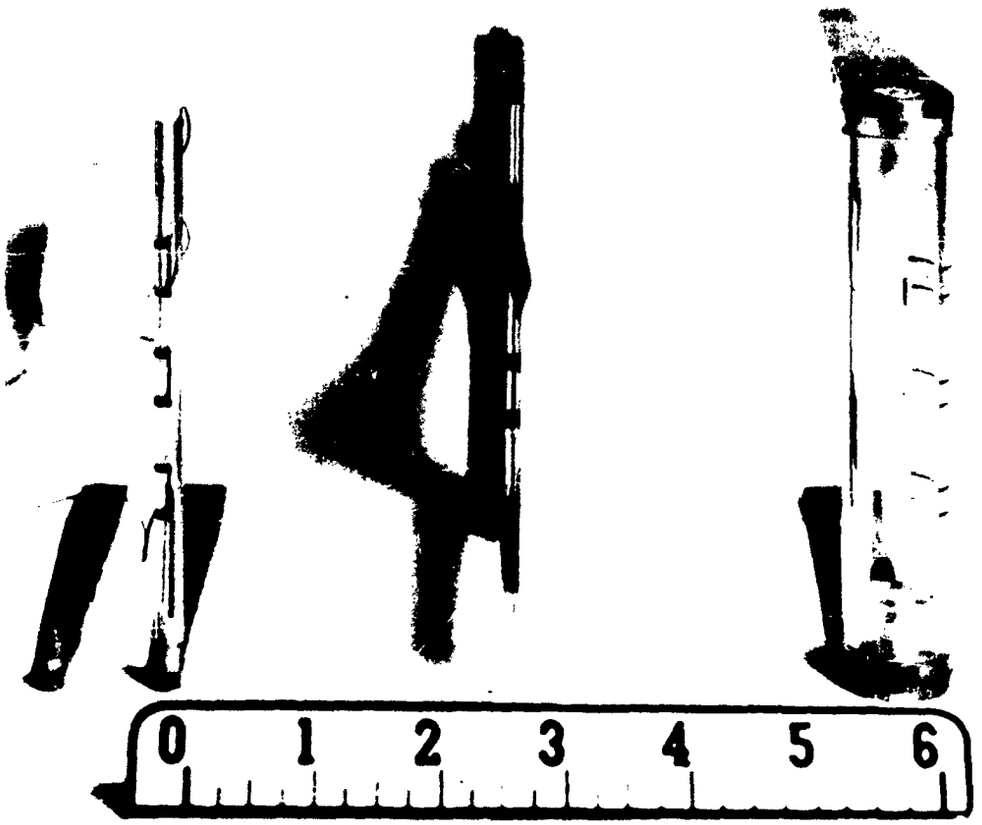

Figure 6 CYLINDRICAL HEAT TRANSFER MODELS

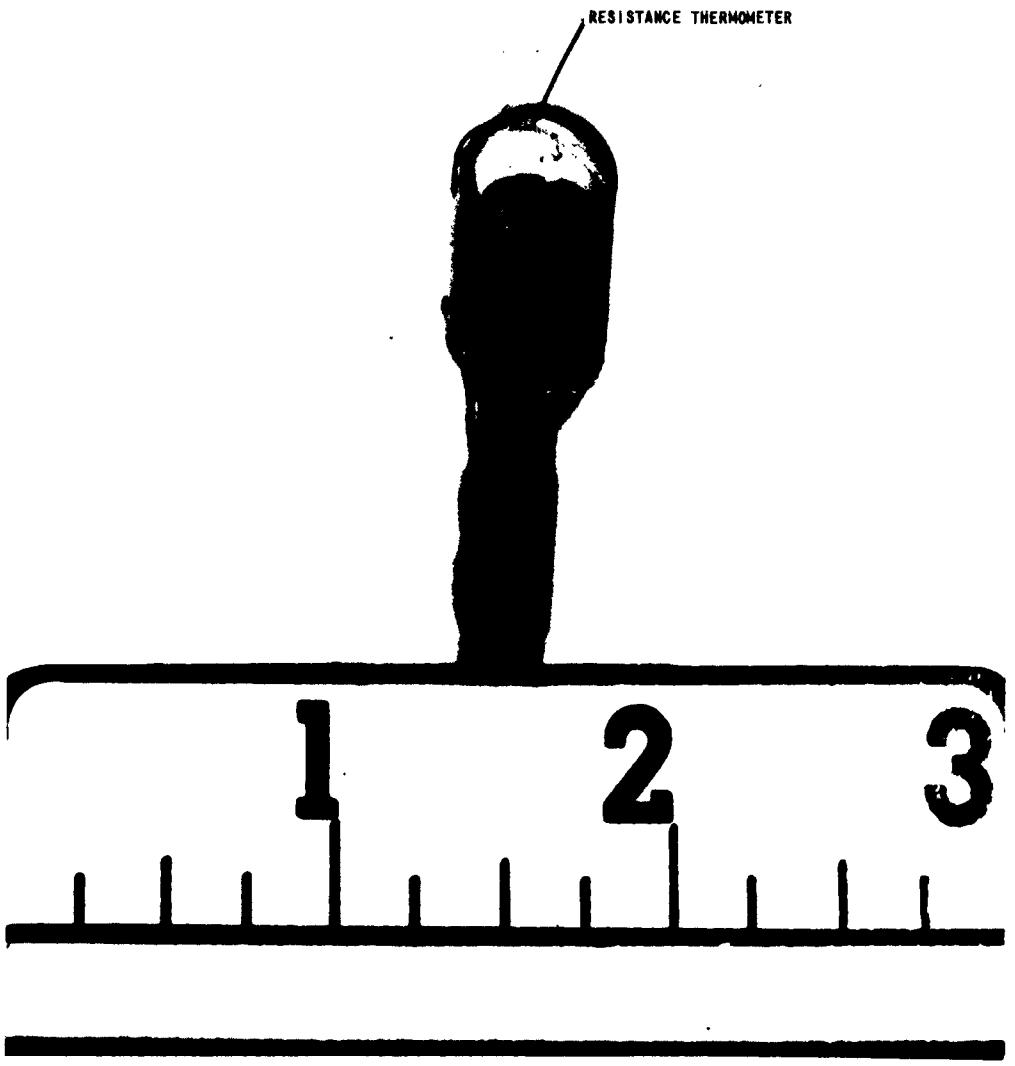

Figure 7 HEMISPHERE CYLINDER HEAT TRANSFER MODEL

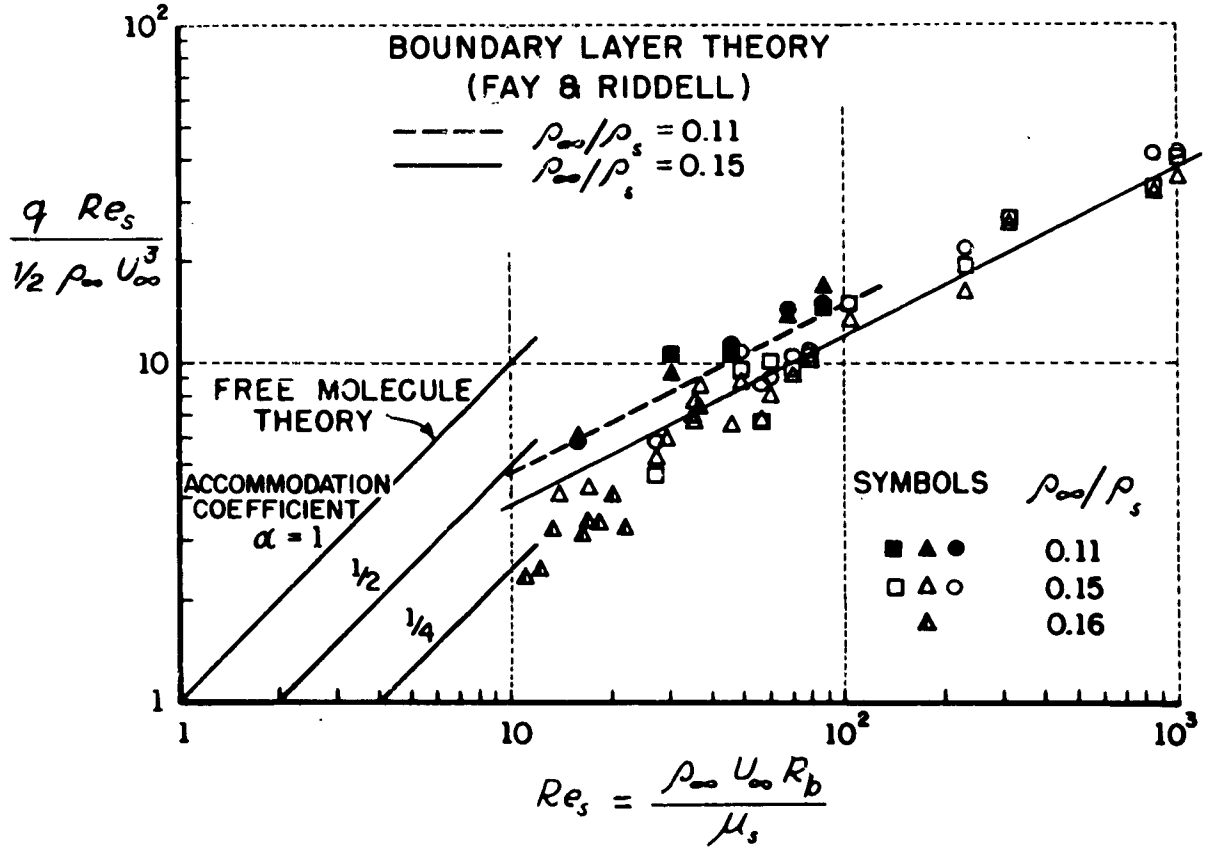

Figure 8 STAGNATION-POINT HEAT TRANSFER TO A TRANSVERSE CYLINDER CORRELATED WITH Re_s

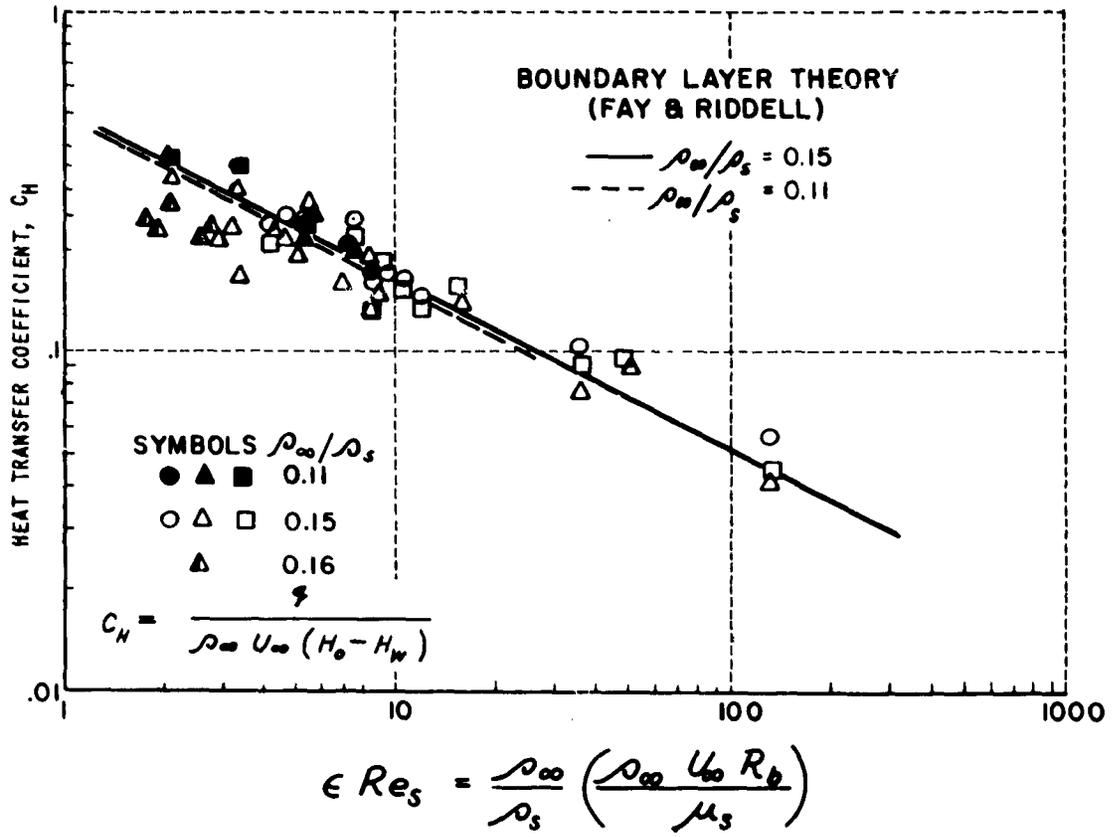

Figure 9 STAGNATION-POINT HEAT TRANSFER TO A TRANSVERSE CYLINDER CORRELATED WITH ϵRe_s

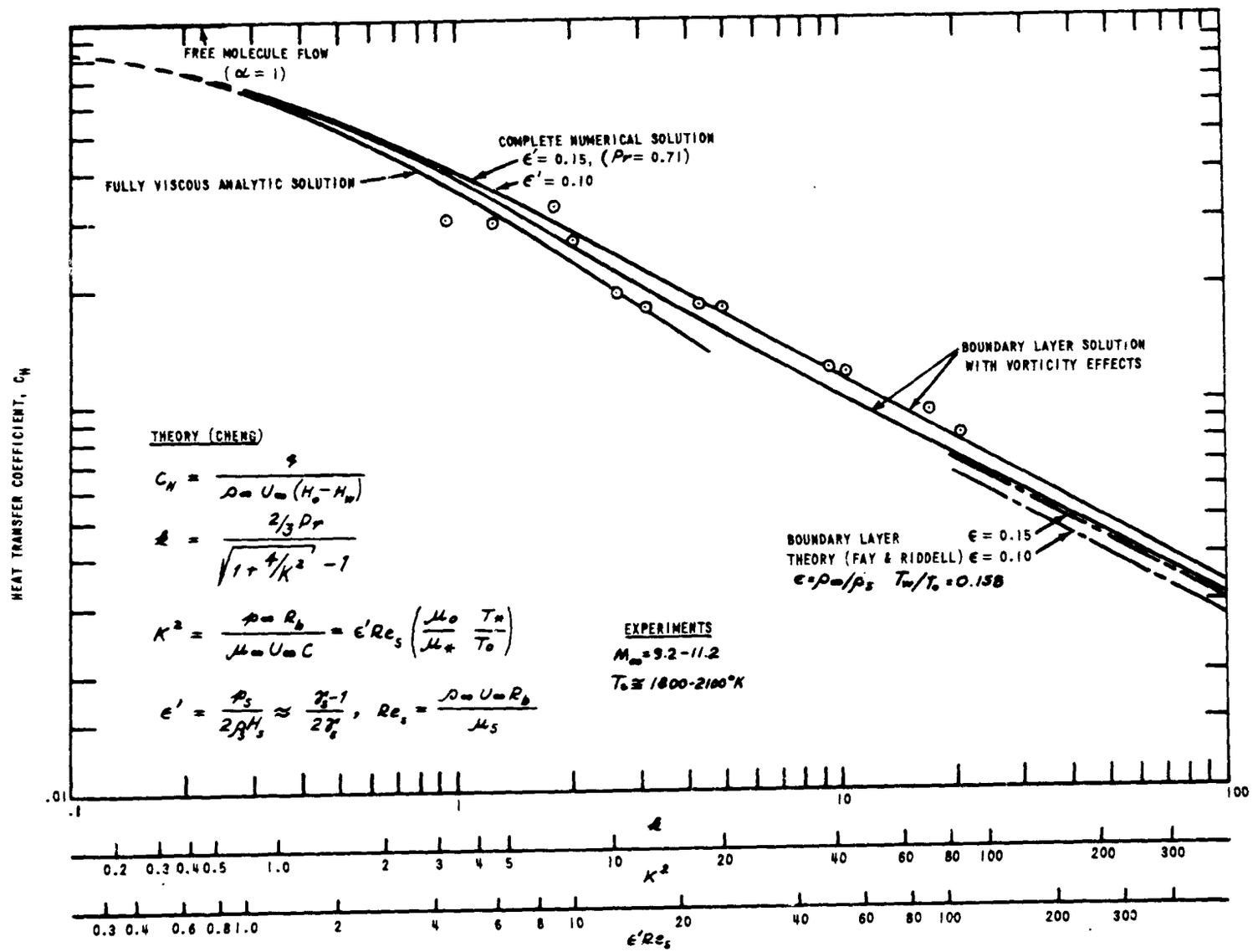

Figure 10 STAGNATION POINT HEAT TRANSFER TO A HEMISPHERE CYLINDER

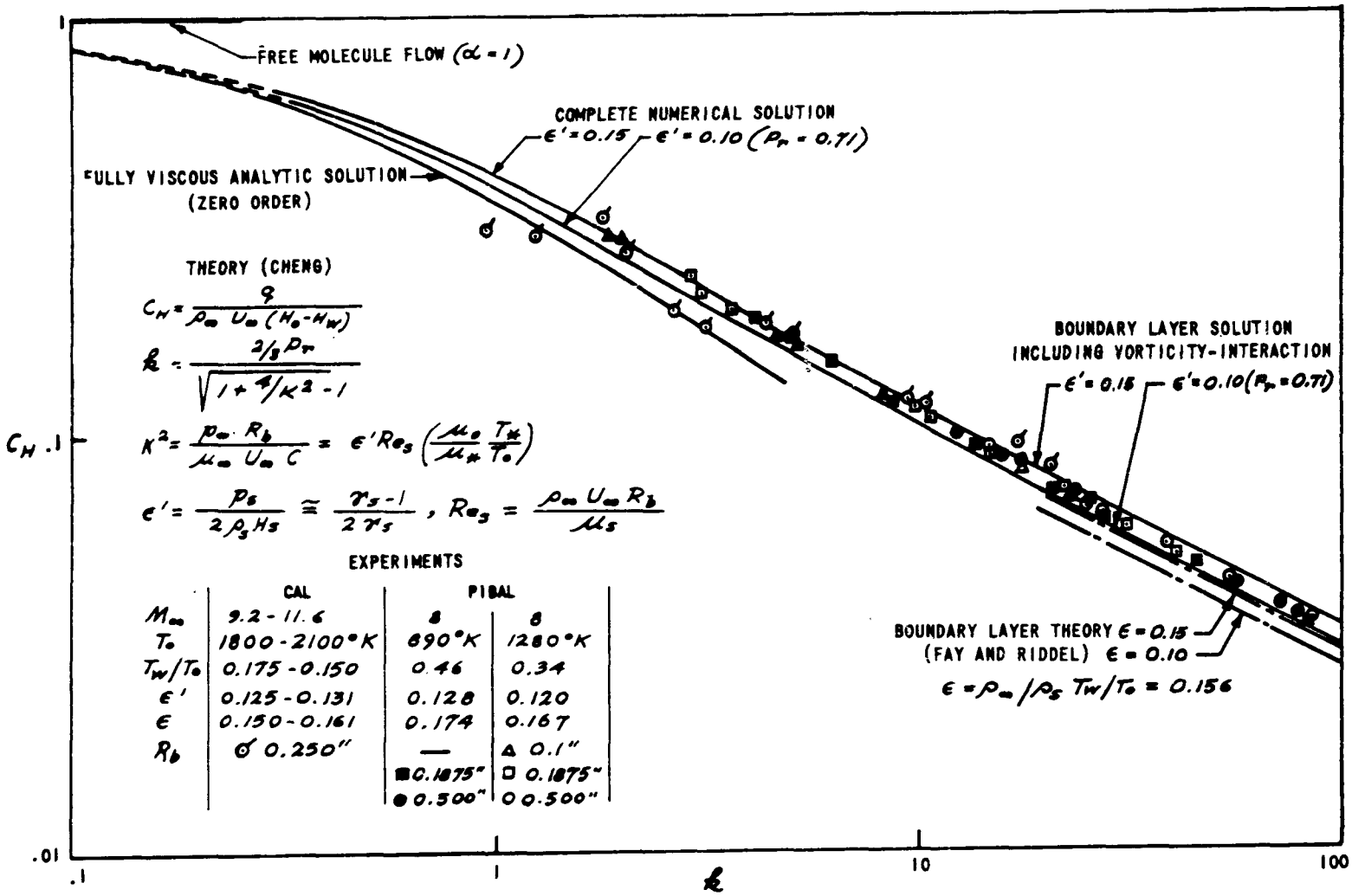

Figure 11 COMPARISON OF CAL AND PIBAL HEMISPHERE-CYLINDER DATA WITH CHENG'S THEORY

UNCLASSIFIED

aligned with the flow. Thin-film resistance thermometers were used to measure the stagnation-point heat-transfer rate. The experimental heat-transfer rates are presented and compared with theoretical predictions. The data obtained with the transverse cylinder are in good agreement with continuum boundary-layer theory at all but the lowest Reynolds numbers. The hemisphere-cylinder data are in good agreement with theoretical analyses accounting for the presence of vorticity-interaction.

UNCLASSIFIED

UNCLASSIFIED

aligned with the flow. Thin-film resistance thermometers were used to measure the stagnation-point heat-transfer rate. The experimental heat-transfer rates are presented and compared with theoretical predictions. The data obtained with the transverse cylinder are in good agreement with continuum boundary-layer theory at all but the lowest Reynolds numbers. The hemisphere-cylinder data are in good agreement with theoretical analyses accounting for the presence of vorticity-interaction.

UNCLASSIFIED

UNCLASSIFIED

aligned with the flow. Thin-film resistance thermometers were used to measure the stagnation-point heat-transfer rate. The experimental heat-transfer rates are presented and compared with theoretical predictions. The data obtained with the transverse cylinder are in good agreement with continuum boundary-layer theory at all but the lowest Reynolds numbers. The hemisphere-cylinder data are in good agreement with theoretical analyses accounting for the presence of vorticity-interaction.

UNCLASSIFIED

UNCLASSIFIED

aligned with the flow. Thin-film resistance thermometers were used to measure the stagnation-point heat-transfer rate. The experimental heat-transfer rates are presented and compared with theoretical predictions. The data obtained with the transverse cylinder are in good agreement with continuum boundary-layer theory at all but the lowest Reynolds numbers. The hemisphere-cylinder data are in good agreement with theoretical analyses accounting for the presence of vorticity-interaction.

UNCLASSIFIED